Ministry for Primary Industries
Manatū Ahu Matua

Acoustic survey of spawning hoki in Cook Strait during winter 2017

New Zealand Fisheries Assessment Report 2018/12

R. L. O'Driscoll
P. Escobar-Flores

ISSN 1179-5352 (online)
ISBN 978-1-77665-841-1 (online)

May 2018

New Zealand Government

Growing and Protecting New Zealand

Requests for further copies should be directed to:

Publications Logistics Officer
Ministry for Primary Industries
PO Box 2526
WELLINGTON 6140

Email: brand@mpi.govt.nz
Telephone: 0800 00 83 33
Facsimile: 04-894 0300

This publication is also available on the Ministry for Primary Industries websites at:
http://www.mpi.govt.nz/news-and-resources/publications
http://fs.fish.govt.nz go to Document library/Research reports

TABLE OF CONTENTS

EXECUTIVE SUMMARY

O'Driscoll, R.L.; Escobar-Flores, P. (2018). Acoustic survey of spawning hoki in Cook Strait during winter 2017.

***New Zealand Fisheries Assessment Report 2018/12*. 39 p.**

An acoustic survey of spawning hoki abundance in Cook Strait was carried out from the research vessel *Ikatere* from 25 July to 27 August 2017 (voyage code IKA1701). Six acoustic snapshots of the main Cook Strait spawning grounds were carried out: five snapshots were completed; but snapshot 2 on 30 July only covered three of the six strata. *Ikatere* is not capable of mark identification trawling, so the only biological data available were from at-sea observers and land-based sampling of the commercial catch. Acoustic estimates of hoki abundance ranged from 51 000 t in snapshot 6 on 26–27 August to 167 000 t in the incomplete snapshot 2 on 30 July (where abundance in the three strata that were not surveyed was assumed to be the average estimate from these strata from the other five snapshots). The average estimate over the six snapshots was 102 000 t. This was half the equivalent estimate from 2015 (204 000 t). The survey weighting (expressed as a coefficient of variation, CV) for the 2017 survey – which includes uncertainty associated with survey timing, sampling precision, acoustic detectability, mark identification, calibration, target strength – was 36%. Only about 54% of the hoki abundance in Cook Strait in 2017 was from hoki school marks. The remaining hoki came from hoki 'fuzz' marks that were also likely to contain other species.

1. INTRODUCTION

Hoki is New Zealand's largest finfish fishery with a total allowable commercial catch (TACC) of 150 000 t in 2016–17 (Ministry for Primary Industries 2017). Although managed as a single stock, hoki are assessed as two stocks, western and eastern. Juveniles from both stocks mix on the Chatham Rise and recruit to their respective stocks as they approach sexual maturity.

The main spawning fisheries for hoki operate from mid-July to late August on the west coast of the South Island (WCSI) and in Cook Strait. Because of the importance of this fishery the hoki stock assessment is updated each year with new information from a wide range of data collection and research programmes.

On the spawning grounds, hoki typically form large midwater aggregations. The occurrence of readily identifiable, single-species aggregations clear of the seabed allows for accurate abundance estimation using acoustics. Acoustic surveys of spawning hoki have been conducted regularly since a 1984 pilot survey of the WCSI spawning grounds (Coombs & Cordue 1995). The results of acoustic surveys of spawning hoki in Cook Strait and the WCSI have been important inputs into hoki stock assessments for 25 years (O'Driscoll 2002a).

Acoustic surveys of the Cook Strait hoki spawning grounds are scheduled every two years to update the biomass indices for the eastern spawning stock. Although the acoustic results from Cook Strait have not been very influential on the results of the stock assessment model, it is considered necessary to monitor the abundance of the eastern spawning stock independently of the Chatham Rise, where both eastern and western hoki are mixed together.

Previous acoustic surveys of Cook Strait were carried out on research vessels annually from 1991–2008 (except 2000, 2004, and 2007). Surveys in 2006 and 2008 also included the east coast South Island areas of Pegasus and Conway Trough (O'Driscoll 2007, 2009). Since 2007, industry vessels have also surveyed part of Cook Strait during the hoki spawning season using the same (NIWA) protocols as for the research vessel surveys (O'Driscoll & Dunford 2008, O'Driscoll & Macaulay 2009, 2010, O'Driscoll 2012, O'Driscoll et al. 2015). The most recent survey was in 2015 (O'Driscoll et al. 2016).

Because MPI was unable to come to a suitable agreement with industry over the provision of a commercial vessel for the 2017 survey (Tiffany Bock, MPI, pers. comm., 30 June 2017), the survey was carried out from the NIWA coastal research vessel *Ikatere*. Although *Ikatere* is not capable of mark identification trawling, it is suitable for carrying out acoustic surveys, ensuring the continuation of the Cook Strait time-series.

1.1 Project objectives

This report fulfils the reporting requirements for Objectives 1 and 2 of Ministry for Primary Industries Research Project HOK2017/01:

1. To continue the time series of relative abundance indices of spawning hoki in Cook Strait using acoustic surveys, with a target coefficient of variation (CV) of the estimate of 30 %.

2. To calibrate acoustic equipment used in the acoustic survey.

2. METHODS

2.1 Survey design

Hoki have a long spawning season, from July to September. It is thought that during the spawning season there is a turnover of fish on the grounds. Therefore, there is no time at which all of the spawning fish are available to be surveyed. The survey design devised to deal with this problem consists of a number of subsurveys or "snapshots" spread over the spawning season. Each snapshot consists of a series of random transects (following the design of Jolly & Hampton (1990)) across strata covering the known distribution of spawning hoki. Estimates of spawning biomass are calculated for each of the snapshots, and these are then averaged to obtain an estimate of the "mean plateau height" (average biomass during the main spawning season). Under various assumptions about the timing and length of the spawning season (Cordue et al. 1992, Coombs & Cordue 1995), estimates of mean plateau height form a valid relative abundance time series.

The stratum boundaries and areas in Cook Strait (Figure 1, Table 1) were the same as in previous surveys, with six main strata (strata 1, 2, 3, 5A, 5B, and 6), covering the areas with depth greater than 200 m (or 180 m in stratum 2). The acoustic survey area in Cook Strait includes grounds which are not commercially fished by the fleet. For example, targeting of hoki by vessels greater than 28 m is not permitted in the Narrows Basin (stratum 1) under the industry agreed Operational Procedures for the Hoki Fishery (version 13), to reduce the catch of small hoki.

2.2 Vessels and equipment

Ikatere is an alloy catamaran launched in 2010, 13.9 m long with a beam of 4.85 m, powered by twin 500 hp Cummins diesels coupled to Hamilton jet units. The vessel has a cruising speed of approximately 24 knots and a top-end speed of about 28 knots. Although *Ikatere* is not permanently fitted with a suitable fisheries echosounder, it has a pole that can be lowered and raised (using a manual winch) through a moon-pool in the centre of the vessel, on which equipment can be fitted when required. For this survey, a Simrad EK60 echosounder with a 38 kHz transducer was fitted to this pole (Figure 2), and lowered to about 1 m below the surface during data acquisition.

An extension of 30 cm was added between the bottom of the retractile pole and the transducer plate between snapshots 2 and 3 on 3 August 2017 (see Figure 2). This extension allowed the transducer to sit deeper below the surface, improving data quality and allowing data to be collected at slightly higher speeds, depending on the conditions.

The acoustic system on *Ikatere* was calibrated in Wellington Harbour before the start of the survey on 20 July 2017, and between snapshots 5 and 6 on 23 August 2017. Calibration reports are provided as Appendices 1 and 2. Both calibrations were of excellent quality and indicated that the echosounder was functioning correctly. The transducer gain of the second calibration was about 0.2 dB higher than that from the first calibration. We used an average of the calibration coefficients from the two calibrations for analysing acoustic data from the 2017 survey (i.e., G_0 = 25.49 dB, sa correction = -0.64 dB).

2.3 Acoustic data collection

The survey objective was to complete 6 snapshots over the survey time window 15 July to 30 August 2017. Assuming a single snapshot would take about 24 hours of survey time, and with *Ikatere* being based in the Evans Bay Marina in the Wellington harbour, the survey approach was to target periods of good weather (at least two consecutive days with less than 15 knots of wind and 1.5 m swell), and survey during the daylight for two consecutive days for up to 12 hours, with the vessel returning to port overnight.

A total of 28 transects were planned across the 6 strata for each snapshot (Table 1), but during the first snapshot it became apparent that this number of transects could not be achieved in two 12-hour days. The number of transects was reduced by one in each of strata 1, 3, and 6 on the second day of snapshot 1 to ensure completion of the snapshot (i.e., giving 25 transects in snapshot 1). Based on the experience gained in the first snapshot, the number of planned transects was reduced from 28 to 23 for the subsequent five snapshots (Table 1). Snapshot 2 was incomplete, with only 3 of the 6 strata surveyed, because adverse weather condition meant that a second day of this snapshot could not be carried out within the required 48 hours. For all remaining snapshots (3, 4, 5, 6), all 23 transects were successfully completed (Table 1).

With the transducer pole lowered in the water, the vessel speed was limited to a maximum of 10 knots, but pre-survey tests showed that data quality at this speed was poor (e.g., high number of ping dropouts and visible mechanical noise at depths greater than 400 m). The most suitable vessel speed for good data quality was between 7–8 knots, although speed was still dependent on the sea state and weather conditions. The pole was raised up during transits and when the distance between acoustic transects was greater than about 2 nautical miles, allowing the vessel to travel at up to 25 knots.

The EK60 echosounder was set-up using scientific 'hoki' settings (power = 2000 W, pulse length = 1.024 ms, ping interval = 2 seconds, see Appendix 1 for more information). Acoustic data were stored onto the echosounder computer and backed up onto a removable USB hard drive. All the acoustic data collection was supervised by Pablo Escobar-Flores, with additional support from Richard O'Driscoll (Snapshot 1) and Alexandre Schimel (first day of Snapshot 3).

2.4 Mark identification trawling

Ikatere was not capable of mark identification trawling, and so the only biological sampling over the survey period was of commercial catches at sea by MPI observers, or on land as part of MPI project HOK2017/02.

2.5 Acoustic data analysis

Acoustic data collected during the survey were analysed using standard echo-integration methods (Simmonds & MacLennan 2005), as implemented in NIWA's ESP3 software package (Ladroit 2017). Echograms were visually examined, and the location of the bottom in each ping determined by a combination of an in-built bottom-echo identification algorithm and manual editing. Regions corresponding to various acoustic mark types were then identified. Marks were classified subjectively (e.g. O'Driscoll 2002b), based on their appearance on the echogram (shape, structure, depth, strength and so on).

Backscatter from marks (regions) identified as hoki was then integrated to produce an estimate of acoustic density, expressed as the mean area backscattering coefficient (s_a, expressed in $m^2\ m^{-2}$, see MacLennan et al. 2002). During integration, acoustic backscatter was corrected for sound absorption by seawater. No CTD profiles were obtained from Cook Strait during the 2017 survey, so the average sound absorption coefficient from the 2015 survey was used instead: 8.93 dB km^{-1} (O'Driscoll et al. 2016).

Acoustic density was output in two ways. First, average acoustic density per transect was calculated. These values were used in abundance estimation (see Section 2.6). Second, acoustic backscatter was integrated over 10-ping bins to produce a series of acoustic density data for each transect. These data series have a high spatial resolution, with each transect being typically made up of 30–100 data values, each value approximately 100 m apart (corresponding to 10 pings). These data are displayed in plots showing the spatial distribution of acoustic density along each transect.

Transect acoustic density estimates were converted to hoki biomass using a ratio, *r*, of mean weight to mean backscattering cross section (linear equivalent of target strength, TS) for hoki. The method of calculating *r* was based on that of O'Driscoll (2002a):

1. using the length frequency distribution of the commercial catch from the year of the survey;

2. using the generic length-weight regression of Francis (2003) to determine mean hoki weight (*w* in kilograms)

$$w = (4.79\times10^{-6})\, L^{2.89} \qquad (1)$$

3. using the most recent TS-length relationship for New Zealand hoki (Dunford et al. 2015):

$$TS = 24.5 \log_{10}(TL) - 83.9 \qquad (2)$$

where *TL* is total fish length in centimetres.

2.6 Abundance estimation

Abundance estimates and variances were obtained for each stratum in each snapshot using the formulae of Jolly & Hampton (1990), as described by Coombs & Cordue (1995). Stratum estimates were combined to produce snapshot estimates, and the snapshots were averaged to obtain the abundance index for 2017.

The sampling precision of the abundance index was calculated in two ways, as described by Cordue & Ballara (2001). The first method was to average the variances from each snapshot. This method potentially underestimates the sampling variance as it accounts only for the observation error in each snapshot. The imprecision introduced by the inherent variability of the abundance in the survey area during the main spawning season is ignored. The second method assumes the snapshot abundance estimates are independent and identically distributed random variables. The sample variance of the snapshot means divided by the number of snapshots is therefore an unbiased estimator of the variance of the index (the mean of the snapshots).

2.7 Survey weighting for stock assessment

The sampling precision will greatly underestimate the overall survey variability, which also includes uncertainty in TS, calibration, and mark identification (Rose et al. 2000). The model weightings (expressed as coefficient of variation or CV) used in the hoki stock assessment model are calculated for individual surveys using a Monte Carlo procedure which incorporates these additional uncertainties (O'Driscoll 2004).

The simulation method used to combine uncertainties and estimate an overall weighting (CV) for each acoustic survey of Cook Strait was described in detail by O'Driscoll (2004), and is summarised below.

Six sources of variance are considered:

- plateau model assumptions about timing and duration of spawning and residence time
- sampling precision
- detectability
- mark identification
- fish weight and target strength
- acoustic calibration

The method has two main steps. First, a probability distribution is created for each of the variables of interest. Second, random samples from each of the probability distributions are selected and combined multiplicatively in Monte Carlo simulations of the process of acoustic abundance estimation.

In each simulation, a biomass model was constructed by randomly selecting values for each variable from the distributions in Table 2. This model was then 'sampled' at dates equivalent to the mid dates of each snapshot (Table 3). The precision of sampling was determined by the snapshot CV, and the biomass adjusted for variability in detectability. The simulated biomass estimate in each snapshot was then split, based on the proportion of acoustic backscatter in 'school' and 'fuzz' marks (see Section 3.3), and mark identification uncertainties applied to each part. The biomass estimates were recombined and calibration and TS uncertainties applied in turn. The same random value for calibration and TS was applied to all snapshots in each simulated 'survey'. Abundance estimates from all snapshot estimates from the simulated survey were averaged to produce an abundance index. This whole process was repeated 1000 times (1000 simulated surveys) and the distribution of the 1000 abundance indices was output. The overall CV was the standard deviation of the 1000 abundance (mean biomass) indices divided by their mean.

3. RESULTS

3.1 2017 commercial fishery

A total catch of 12 718 t was taken from Cook Strait between 1 June and 30 September 2017, with most hoki caught between 15 July and 15 September (Figure 3). The acoustic survey was within the period of high catches. The hoki length frequency distribution from the 2017 commercial fishery in Cook Strait based on scientific observer data, and land-based sampling is shown in Figure 4. The mean length of hoki was 79.1 cm. Mean weight and mean backscattering cross-section (obtained by transforming the scaled length frequency distribution in Figure 4 by equations (1) and (2) and then calculating the means of the transformed distributions) were 1.55 kg and 0.000189 m^2 (equivalent to –37.2 dB) respectively, giving a ratio, *r*, for Cook Strait in 2017 of 8206 kg m^{-2}.

3.2 Acoustic data collection

Six acoustic snapshots of the main Cook Strait spawning grounds were carried out from 25 July to 27 August 2017 (Table 3). The six snapshots were spaced evenly across the hoki spawning period.

The survey demonstrated that acoustic data could be successfully collected in Cook Strait using the *Ikatere* in up to 20 knots of wind and swell heights of 1.5 m. Of the 6 snapshots planned, only one could not be completed in time due to adverse weather. Data quality was generally acceptable, but there were examples of missing pings or interference from wave-generated bubbles, (e.g., Figure 5 and subsequent echograms). The effective range of the echosounder system on *Ikatere* was about 600 m. Below this depth, flow- and vessel-induced noise, meant that the signal-to-noise ratio decreased (e.g., Figure 6). As almost all hoki marks were shallower than 600 m (see Section 3.3), this did not affect survey results.

3.3 Mark identification

Marks in Cook Strait were similar to those observed in previous surveys from 2001–15. Example echograms of some of these mark types are shown in Figures 5–12. Further examples are provided by O'Driscoll (2002b, 2003, 2007, 2009, 2012), O'Driscoll & Dunford (2008), O'Driscoll & Macaulay (2009, 2010), and O'Driscoll et al. (2015, 2016).

1. Hoki schools ("hok")
Hoki school marks were characterised by relatively high acoustic return, with clearly defined edges, typically occurring at 200–500 m water depth, and often in midwater over canyon features. The densest hoki schools were observed in Cook Strait Canyon (strata 2 and 5A) during snapshots 2 and 5 (e.g., Figure 7), but hoki schools were also occasionally observed in the deep water between Cook Strait and Wairarapa Canyons (stratum 5B, e.g., Figure 6), in the Narrows Basin (stratum 1, e.g., Figure 8), and in Nicholson Canyon (stratum 3). In the past, commercial and research trawling on hoki schools has typically caught 90–100% hoki by weight.

2. Hoki bottom fuzz ("bmix")
Hoki bottom fuzz marks were diffuse, low-density layers adjoining the seabed, and extending more than 50 m above it. These were usually in water depths shallower than 300 m. This mark type was commonly observed in the Narrows Basin (e.g., Figures 8–9) and over the Terawhiti Sill (stratum 6). Previous mark identification trawls on hoki bottom fuzz have caught variable proportions of hoki by weight (10–100% hoki).

3. Hoki pelagic fuzz ("pmix")
Hoki pelagic fuzz marks were characterised by low acoustic return, relatively constant depth within the 200–600 m range, typically over deep waters (500–1000 m), and often showing single target echoes within the layers. In 2017, these marks were common in outer Cook Strait Canyon (e.g., Figure 10), in the deep water between Cook and Wairarapa Canyons (e.g., Figure 6), in Nicholson Canyon (e.g., Figure 11), and associated with hoki school marks in Cook Strait Canyon (e.g., Figure 7). Previous mark identification trawls on hoki pelagic fuzz have typically caught 60–100% hoki by weight.

4. Bottom non-hoki ("b")
Bottom non-hoki marks were bottom-referenced layers or schools, which were typically denser and shallower (less than 200 m depth) than hoki bottom fuzz layers. Bottom non-hoki marks were observed on one transect in 2017 in the Narrows Basin (Figure 12). Previous research trawling on this mark type caught less than 10% hoki, with catches typically dominated by ling, however the marks seen in 2017 could also be jack mackerel.

5. Jack mackerel ("jma")
Jack mackerel marks were observed as strong surface-referenced layers consisting of small schools and strong single targets at depths of 50 to 200 m. As in previous surveys, jack mackerel marks were usually observed in the Narrows Basin (e.g., Figure 8). Previous research trawling on this mark type caught mainly jack mackerel and few hoki.

6. Mesopelagic layers ('p")
Mesopelagic layers were strongly surface-referenced marks usually occurring between 0 and 300 m depth, and exhibiting strong diurnal vertical migration patterns. Mesopelagic layers were widespread throughout the survey areas (e.g., Figures 5–7, 10). Targeted trawling on this mark type in the past only caught a few very small (less than 30 cm) hoki.

7. Spiny dogfish ("spd")
Spiny dogfish marks were characteristically surface-referenced marks similar to jack mackerel marks, and consisted of small schools and single targets at depths of 100–200 m, above hoki schools. Midwater spiny dogfish marks are sometimes observed in Cook Strait Canyon, but were not conspicuous during the 2017 survey. Livingston (1990) found that midwater aggregations of spiny dogfish above hoki schools were feeding on recently spawned hoki eggs.

Acoustic backscatter from regions corresponding to hoki schools, hoki bottom fuzz, and hoki pelagic fuzz were integrated to obtain acoustic density estimates, even though it is known that hoki fuzz marks also contain a proportion of other species. This is consistent with data analysis practice from previous years (O'Driscoll 2002a). No species decomposition of acoustic backscatter in mixed layers was attempted because of the absence of mark identification trawling in this 2017 survey. If there was a change in the

proportion of hoki in fuzz marks over time (as suggested by O'Driscoll (2006) for bottom fuzz marks), this approach will lead to a bias in the relative abundance estimates. However, the Monte Carlo estimation of survey uncertainty will incorporate some of this potential bias because the lognormal distribution of uncertainty associated with species mix is very broad (see Table 2). In Section 3.5, abundance estimates are presented for hoki school marks only (where mark identification is relatively certain), as well as for the combination of hoki school and hoki fuzz marks.

3.4 Distribution of hoki backscatter

Expanding symbol plots show the spatial distribution of hoki backscatter density along each transect for each of the six snapshots of the 2017 Cook Strait survey (Figure 13). The distribution of hoki in Cook Strait was generally similar to that observed in previous research and industry surveys between 2001 and 2015 (O'Driscoll 2002b, 2003, 2006, 2007, 2009, 2012, O'Driscoll & McMillan 2004, O'Driscoll & Dunford 2008, O'Driscoll & Macaulay 2009, 2010, O'Driscoll et al. 2015, 2016). Hoki densities were highest in Cook Strait Canyon (strata 2 and 5A) with peak densities in snapshots 2 and 5 (see example in Figure 7).

Most of the acoustic backscatter in the deep water between Cook Strait and Wairarapa Canyons (stratum 5B) and in Nicholson Canyon (stratum 3) came from pelagic fuzz marks and densities in these areas were relatively low (Figure 13). Acoustic densities were also generally low in the Narrows Basin (stratum 1) and over the Terawhiti Sill (stratum 6), and most of the backscatter from these areas was from bottom fuzz marks. Densities were relatively low in all strata in snapshots 3, 4, and 6 (Figure 13).

3.5 Hoki abundance estimates

Hoki abundance estimates by snapshot and strata are given in Table 4, and estimates by snapshot and mark type are plotted in Figure 14. Estimates of hoki abundance in the six snapshots using the value of r calculated for 2017 ranged from 51 000 t (CV 13%) in snapshot 6 on 26–27 August to 167 000 t (CV 51%) in the incomplete snapshot 2 on 30 July (where abundance in the three strata which were not surveyed was assumed to be the average estimate from these strata from the other five snapshots). The CV for snapshot 2 was high because 60% of the estimated biomass came from one transect with particularly strong marks (see Figure 7). Abundance estimates in snapshot 3 on 4–5 August and snapshot 4 on 10–11 August were relatively low, at a time when abundance often peaked in previous years (Figure 15). There was also a large decrease in observed abundance between snapshot 5 on 18–19 August and snapshot 6 (see Figure 14). Differences between individual snapshots are probably due to sampling variability (transect location and fish behaviour) as well as changes in abundance. High variability in abundance between snapshots was observed in previous surveys, in 2006, 2007, 2011, 2013, and 2015 (Figure 15).

When results from Table 4 were averaged over the six snapshots, 62% of the estimated hoki biomass was in stratum 2, 11% in stratum 1, 10% in stratum 5B, 8% in stratum 5A, 3% in stratum 3, and 2% in stratum 6. Hoki densities in strata 1 and 5B were generally low (see Figure 13), and the important contribution of these strata to the overall biomass was due to their relatively larger areas. The contribution of biomass from outside Cook Strait Canyon may also be overestimated because most of the estimated biomass in the other strata was from hoki fuzz marks, which tend to contain other species (Table 5).

The average proportion of the estimated biomass from hoki school marks in 2017 was 54% (Table 5). This was lower than the proportion in school marks in 2015 (73%) and 2013 (78%), but within the range of proportions in previous surveys (30–74% of hoki in school marks in 1991–2011). Most (88%) of the hoki observed in stratum 2 were in school marks (Table 5). Hoki school marks were also observed occasionally in strata 1, 3, 5A, and 5B. As in previous surveys, changes in abundance over the survey period were driven mainly by changes in the biomass of hoki school marks (see Figure 14). The biomass from hoki fuzz marks remained relatively constant between 32 000 and 50 000 t in snapshots 1–6.

The mean abundance from snapshots 1–6 was 102 000 t (see Table 4). The average of the snapshot coefficients of variation was 15%. The variance of the abundance estimates from the six snapshots was 17%. The similarity of the two estimates of sampling variance provides evidence that variation in estimated biomass between individual snapshots was consistent with sampling variability.

3.6 Survey weighting for stock assessment

The overall survey weighting estimated from the Monte Carlo simulation model for Cook Strait was 36% (Table 6). As in previous Cook Strait surveys (O'Driscoll 2004), timing (including uncertainties about plateau timing and residence time), sampling error, and mark identification were the major sources of uncertainty (Table 6). Uncertainties due to calibration, detectability, and TS contributed relatively little to the overall CV. However, incorrect choice of TS and calibration coefficients have the potential to introduce bias in estimates, which is not reflected in the CV in Table 6.

4. DISCUSSION

Six acoustic snapshots of the Cook Strait spawning grounds were carried out from the coastal research vessel *Ikatere* during winter 2017. The use of *Ikatere* to carry out the survey was due to the unavailability of commercial fishing vessels, which have carried out surveys from 2007–15. By using a pole-mounted transducer, acoustic data were successfully collected in up to 20 knots of wind and swell heights of 1.5 m. Due to the requirement to return the vessel to Wellington overnight, the number of transects had to be reduced from 28 to 23 to allow each snapshot to be completed within two consecutive days of 12-hours. This survey strategy also required the weather to remain suitable for 36 hours to allow a snapshot to be completed. Snapshot 2 was only partially completed (three of six strata) because the weather deteriorated after the first day of survey.

Despite these limitations, the survey was deemed suitable for estimating hoki abundance, with the six snapshots spread relatively evenly over the survey period (see Figure 15), within the timing of peak commercial catches (see Figure 3), and with suitable precision (sampling CV = 17%, which was well below the target CV of 30%). We conclude that the *Ikatere* provides a suitable alternative to the use of commercial vessels and larger research vessels (e.g., *Kaharoa*) for future acoustic surveys of Cook Strait hoki.

The major disadvantage of using *Ikatere* was the lack of targeted mark identification trawls. This was also identified as an issue for previous industry vessel surveys in 2007 and 2009 (O'Driscoll & Macaulay 2009). Regular sampling of all mark types is important to understand species composition, especially as this can change over time (e.g., O'Driscoll 2007). This is particularly important for hoki fuzz marks, which typically contribute 30–50% of the hoki biomass in Cook Strait, but which are not usually targeted commercially because of low fish density. If the *Ikatere* is used for future surveys, we recommend that another "catcher" vessel (either commercial or research) is also used to carry out directed mark-identification trawling.

The abundance index for 2017, calculated using the length frequency from the 2017 commercial fishery and the latest TS-length relationship, was 102 000 t, which was half of the estimate from the previous survey in 2015 (204 000 t), and the lowest estimate since 2008 (Table 7). The overall CV of the 2017 estimate (36%) was within the range of estimated uncertainty in research and industry vessel surveys since 2001 (CV 30–46%), reflecting the consistent survey design and execution over this period.

The apparent large decrease in hoki abundance in Cook Strait between 2015 and 2017 is not consistent with predictions from the most recent hoki stock assessment, which suggests that the spawning biomass of the eastern hoki stock is increasing or stable and above target levels (Ministry for Primary Industries 2017). It

was particularly surprising to observe low abundance in Cook Strait in the first two weeks of August (snapshots 3 and 4 in 2017) as this is when the abundance often peaked in previous surveys (see Figure 15).

5. ACKNOWLEDGMENTS

Thanks to the skippers Andrew James, Bryce Bennett and Graeme Bennett, as well as the mates John Hadfield, Rob Stewart, Peter Wall and Rodney Niven for their assistance on carrying out the survey on *Ikatere*. Thanks also to John Hadfield and Greg Foothead for the logistic support. The survey was funded by Ministry for Primary Industries research project HOK2017/01. Alexandre Schimel reviewed a draft of this report.

6. REFERENCES

Coombs, R.F.; Cordue, P.L. (1995). Evolution of a stock assessment tool: acoustic surveys of spawning hoki (*Macruronus novaezelandiae*) off the west coast of South Island, New Zealand, 1985–91. *New Zealand Journal of Marine and Freshwater Research 29*: 175–194.

Cordue, P.L.; Ballara, S.L. (2001). An acoustic survey of spawning hoki in Cook Strait during winter 1999. *New Zealand Fisheries Assessment Report 2001/15*. 18 p.

Cordue, P.L.; McAllister, M.K.; Pikitch, E.K.; Sullivan, K.J. (1992). Stock assessment of hoki 1991. New Zealand Fisheries Assessment Research Document 92/10. 41 p. (Unpublished report held by NIWA library, Wellington.)

Demer, D.A.; Berger, L.; Bernasconi, M.; Bethke, E.; Boswell, K.; Chu, D.; Domokos, R.; et al. (2015). Calibration of acoustic instruments. *ICES Cooperative Research Report No. 326*. 133 p.

Doonan, I.J.; Coombs, R.F.; McClatchie, S. (2003). The absorption of sound in seawater in relation to the estimation of deep-water fish biomass. *ICES Journal of Marine Science 60*: 1047–1055.

Dunford, A.J.; O'Driscoll, R.L.; Oeffner, J. (2015). Improvements in estimating an acoustic target strength-length relationship for hoki (*Macruronus novaezelandiae*). *Fisheries Research 162:*12–19.

Fofonoff, P.; Millard, R., Jr (1983). Algorithms for computation of fundamental properties of seawater. *UNESCO Technical Papers in Marine Science 44*. 53 p.

Francis, R.I.C.C. (2003). Analyses supporting the 2002 stock assessment of hoki. *New Zealand Fisheries Assessment Report 2003/5*. 34 p.

Jolly, G.M.; Hampton, I. (1990). A stratified random transect design for acoustic surveys of fish stocks. *Canadian Journal of Fisheries and Aquatic Sciences 47*: 1282–1291.

Ladroit, Y. (2017). ESP3: an open-source software for fisheries acoustic data processing. https://bitbucket.org/echoanalysis/esp3

Livingston, M.E. (1990). Spawning hoki (*Macruronus novaezelandae* Hector) concentrations in Cook Strait and off the east coast of the South Island, New Zealand, August–September 1987. *New Zealand Journal of Marine and Freshwater Research 24*: 503–517.

MacLennan, D.N.; Fernandes P.G.; Dalen J. (2002). A consistent approach to definitions and symbols in fisheries acoustics. *ICES Journal of Marine Science 59*:365–369.

Ministry for Primary Industries (2017). Fisheries Assessment Plenary, May 2017: stock assessments and stock status. Compiled by the Fisheries Science Group, Ministry for Primary Industries, Wellington, New Zealand. 1596 p.

O'Driscoll, R.L. (2002a). Review of acoustic data inputs for the 2002 hoki stock assessment. *New Zealand Fisheries Assessment Report 2002/36*. 64 p.

O'Driscoll, R.L. (2002b). Acoustic survey of spawning hoki in Cook Strait during winter 2001. *New Zealand Fisheries Assessment Report 2002/37*. 35 p.

O'Driscoll, R.L. (2003). Acoustic survey of spawning hoki in Cook Strait during winter 2002. *New Zealand Fisheries Assessment Report 2003/27*. 34 p.

O'Driscoll, R.L. (2004). Estimating uncertainty associated with acoustic surveys of spawning hoki (*Macruronus novaezelandiae*) in Cook Strait, New Zealand. *ICES Journal of Marine Science 61*: 84–97.

O'Driscoll, R.L. (2006). Acoustic survey of spawning hoki in Cook Strait during winter 2005, and revision of hoki acoustic abundance indices for Cook Strait and the west coast South Island. *New Zealand Fisheries Assessment Report 2006/44*. 46 p.

O'Driscoll, R.L. (2007). Acoustic survey of spawning hoki in Cook Strait and off the east coast South Island during winter 2006. *New Zealand Fisheries Assessment Report 2007/21*. 52 p.

O'Driscoll, R.L. (2009). Acoustic survey of spawning hoki in Cook Strait and off the east coast South Island during winter 2008. *New Zealand Fisheries Assessment Report 2009/17*. 52 p.

O'Driscoll, R.L. (2012). Acoustic survey of spawning hoki in Cook Strait during winter 2011. *New Zealand Fisheries Assessment Report 2012/17*. 50 p.

O'Driscoll, R.L.; Dunford, A.J. (2008). Acoustic survey of spawning hoki in Cook Strait during winter 2007. NIWA Client Report WLG2008-1 for The Deepwater Group Ltd. 44 p.

O'Driscoll, R.L.; Ladroit, Y.; Dunford, A.J.: MacGibbon, D.J. (2015). Acoustic survey of spawning hoki in Cook Strait and Pegasus Canyon during winter 2013. *New Zealand Fisheries Assessment Report 2015/04*. 51 p.

O'Driscoll, R.L.; Ladroit, Y.; Dunford, A.J.: MacGibbon, D.J. (2016). Acoustic survey of spawning hoki in Cook Strait during winter 2015 and update of acoustic q priors for hoki stock assessment modelling. *New Zealand Fisheries Assessment Report 2016/44*. 55 p.

O'Driscoll, R.L.; Macaulay, G.J. (2009). Industry acoustic survey of spawning hoki in Cook Strait during winter 2008. NIWA Client Report WLG2009-8 for The Deepwater Group Ltd. 40 p.

O'Driscoll, R.L.; Macaulay, G.J. (2010). Industry acoustic survey of spawning hoki in Cook Strait during winter 2009. NIWA Client Report WLG2010-13 for The Deepwater Group Ltd. 56 p.

O'Driscoll, R.L.; McMillan, P.J. (2004). Acoustic survey of spawning hoki in Cook Strait during winter 2003. *New Zealand Fisheries Assessment Report 2004/20*. 39 p.

Rose, G.; Gauthier, S.; Lawson, G. (2000). Acoustic surveys in the full monte: simulating uncertainty. *Aquatic Living Resources 13*: 367–372.

Simmonds, E.J.; MacLennan, D.N. (2005). Fisheries acoustics. Second edition. Blackwell Science, Oxford. 437 p.

7. TABLES

Table 1: Planned transect allocation and transects achieved in the 2017 acoustic survey of spawning hoki in Cook Strait. Stratum locations are shown in Figure 1.

Stratum	Name	Boundary	Area (km^2)	No. of planned transects	No. of transects in snapshot 1	No. of transects in snapshot 2	No. of transects in snapshot 3–6
1	Narrows Basin	200–200 m	330	4	3	0	4
2	Cook Strait Canyon	180–180 m	220	9	9	7	7
3	Nicholson Canyon	200–200 m	55	4	3	0	3
5A	Cook Strait Canyon extension	position to 200 m	90	4	4	0	3
5B	Deep water	position to 200 m	215	3	3	3	3
6	Terawhiti Sill	200–200 m	65	4	3	3	3
			Total	28	25	13	23

Table 2: Values of parameters and their distributions used in Monte Carlo uncertainty simulations to determine model weighting (from O'Driscoll 2004).

Term	Notation	Distribution	Values*
Mean arrival date	$\bar{d}$	Uniform	1 July–9 August
Mean residence time	$\bar{r}$	Uniform	24–47 days
Individual arrival date	d_i	Normal	$\bar{d}$ (5 days)
Individual residence time	r_i	Normal	$\bar{r}$ (10 days)
Sampling	s	Normal	1.0 (snapshot CV)
Detectability	D	Uniform	0.85–0.97
Mark identification – 'fuzz' marks	Id_{fuzz}	Lognormal	0.78 (0.72)
Mark identification – 'school' marks	Id_{school}	Lognormal	0.10 (0.16)
Calibration	cal	Uniform	cal ± 0.2 dB
Target strength[+]	TS	Uniform	TS ± 0.5 dB

* For uniform distribution, values are ranges; for normal distributions, values are means with standard deviations (in parentheses); for lognormal distributions, values are the mean and standard deviation (in parentheses) of $\log_e$(variable).

[+] Uncertainty associated with TS arose from variation in fish size, and from differences in the slope of alternative TS-length relationships. Potential bias due to differences in the intercept of alternative TS-length models was ignored because it will not affect the relative values of acoustic indices (see O'Driscoll 2004 for details).

Table 3: Summary of snapshots carried out during the 2017 Cook Strait hoki acoustic survey. Times are NZST.

Snapshot	Start time	End time	No. of transects
1	25 Jul 08:17	26 Jul 17:25	25
2	30 Jul 07:30	30 Jul 17:16	13
3	04 Aug 08:17	05 Aug 17:52	23
4	10 Aug 07:33	11 Aug 18:09	23
5	18 Aug 09:13	19 Aug 17:55	23
6	26 Aug 07:57	27 Aug 15:30	23

Table 4: Hoki acoustic abundance estimates from the 2017 Cook Strait survey by snapshot and stratum. Mean is the average biomass per stratum over all snapshots. NA indicates strata that were not surveyed. *Total biomass in snapshot 2 was estimated by assuming abundance in the three strata which were not surveyed was the average estimate from these strata from the other five snapshots.

	Stratum biomass ('000 t)						Total	Snapshot
Snapshot	1	2	3	5A	5B	6	('000 t)	CV
1	6	97	4	7	5	2	121	23
2	NA	125	NA	11	NA	1	167*	51
3	22	25	3	7	14	2	74	14
4	25	40	3	3	9	1	81	16
5	13	67	4	15	11	5	116	18
6	8	21	2	6	14	1	51	13
Mean	15	63	3	8	11	2	102	15

Table 5: Percentage of the hoki abundance estimate from hoki school marks in each snapshot and strata for the 2017 Cook Strait survey. Percentages were calculated in relation to abundance estimates in Table 4.

	Percentage of biomass in hoki school marks						
Snapshot	1	2	3	5A	5B	6	Overall
1	0	92	0	0	0	0	73
2	0	97	0	54	0	0	76
3	14	77	0	19	0	0	32
4	0	91	29	0	0	0	46
5	0	85	0	48	44	0	60
6	0	85	0	0	0	0	35
Mean	2	88	5	20	7	0	54

Table 6: Results of Monte Carlo simulations to determine model weighting for the 2017 Cook Strait acoustic survey (see O'Driscoll 2004 for details). The CV for the survey is given in a stepwise cumulative fashion to allow the contribution of each component of the abundance estimation process to be assessed. 'Timing' refers to uncertainties associated with the timing of snapshots relative to the plateau height model and includes uncertainties associated with assumptions about fish arrival date and residence time.

Timing	0.233
+ Sampling	0.259
+ Detectability	0.261
+ Mark identification	0.350
+ Calibration	0.352
+ TS	0.355
Total	0.355

Table 7: Acoustic indices of hoki abundance for Cook Strait 1988–2017. All indices re-calculated for this report using the acoustic TS derived from commercial length frequency data in each survey year using the most recent hoki TS-length relationship of Dunford et al. (2015) (see O'Driscoll et al. 2016). The 2017 estimate is the mean of snapshots 1–6.

Year	No of accepted snapshots	Biomass ('000 t)	CV
1991	4	88	0.41
1993	4	283	0.52
1994	3	278	0.91
1995	4	194	0.61
1996	5	92	0.57
1997	6	141	0.40
1998	5	80	0.44
1999	6	114	0.36
2001	11	102	0.30
2002	9	145	0.35
2003	9	104	0.34
2005	9	59	0.32
2006	7	60	0.34
2007*	4	104	0.46
2008	7	82	0.30
2009*	5	166	0.39
2011*	6	141	0.35
2013*	7	168	0.30
2015*	5	204	0.33
2017	6	102	0.36

* Surveys from industry vessels.

8. FIGURES

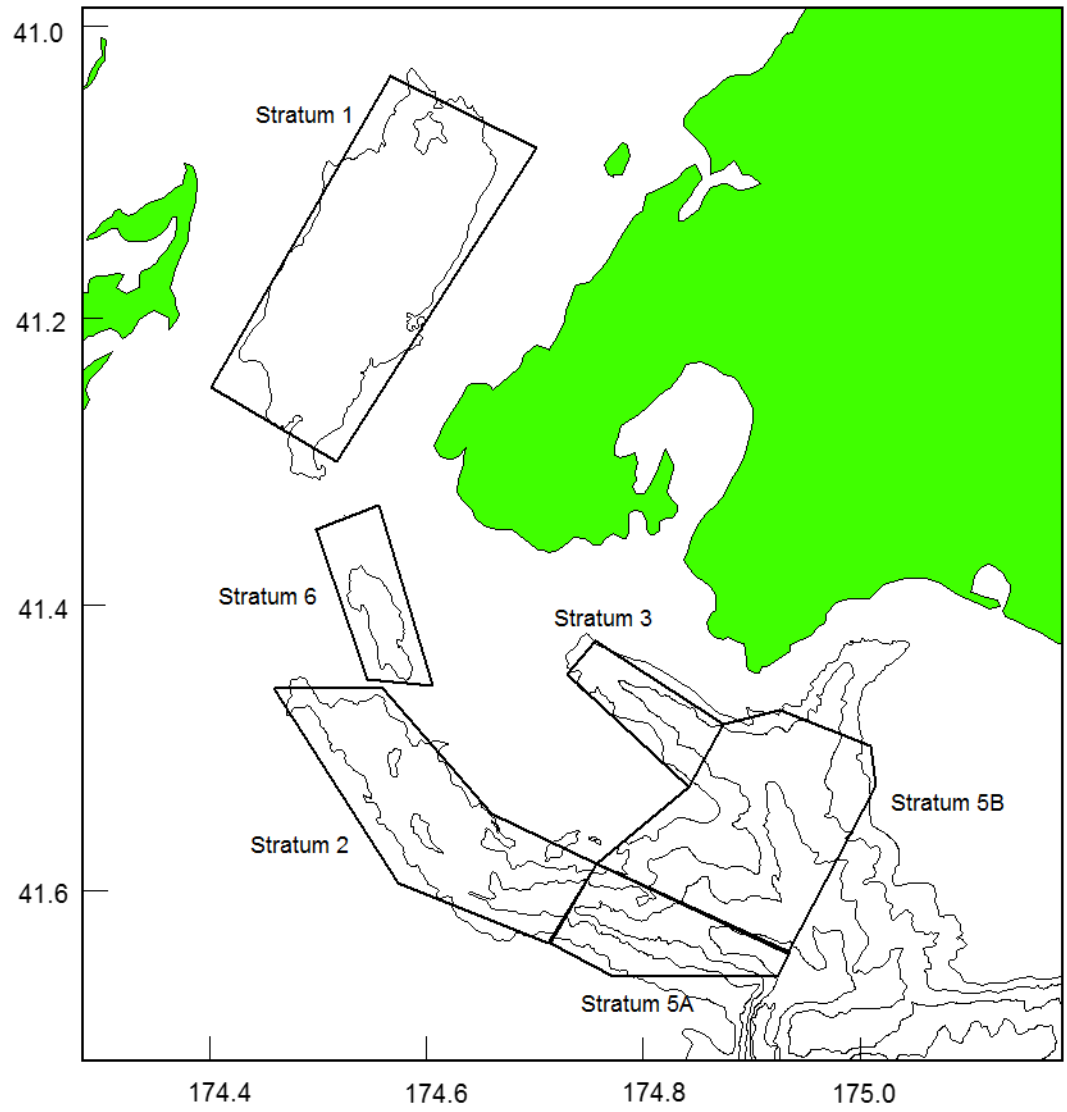

Figure 1: Stratum boundaries for the 2017 acoustic survey of Cook Strait spawning hoki: 1, Narrows Basin; 2, Cook Strait Canyon; 3, Nicholson Canyon; 5A, Cook Strait Canyon extension; 5B, Deepwater outside Nicholson and Wairarapa Canyons; 6, Terawhiti Sill. Depth contours are 250, 500, 750, and 1000 m.

Figure 2: Pictures showing the location of the pole and moon pool on *Ikatere*'s (left upper panel), and the 38 kHz transducer mounted at the bottom of the pole using a stainless-steel plate (right upper panel). The lower panel shows the pole extension (about 30 cm long) that was added between the pole and the stainless-steel plate on 3 August 2017.

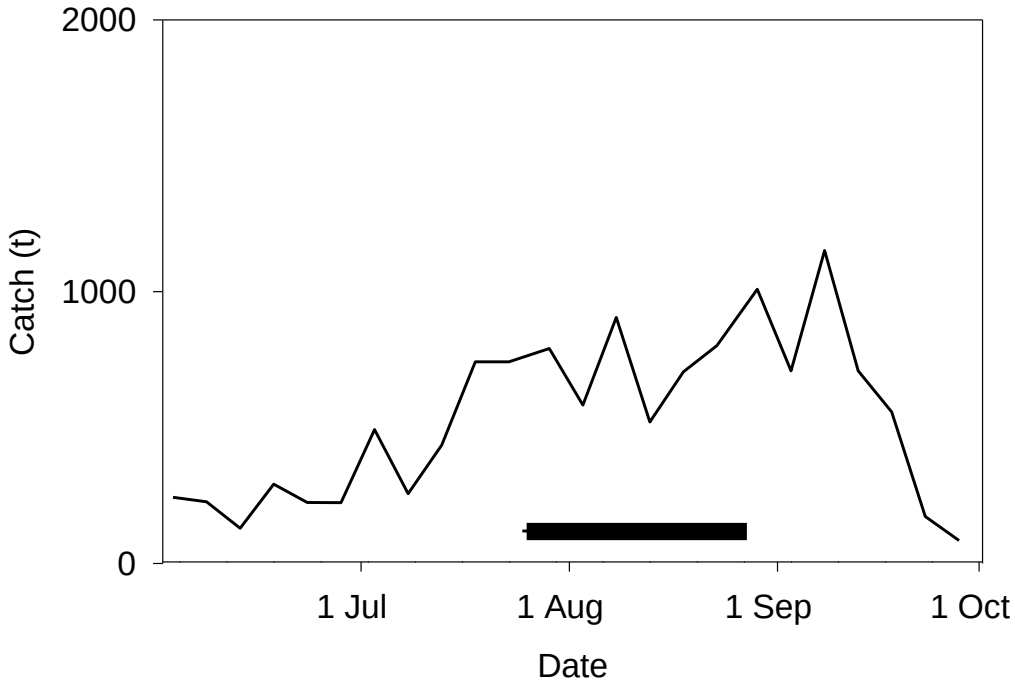

Figure 3: Timing of acoustic survey in 2017 (bar along the x axis) in relation to the commercial hoki catch from Cook Strait in 5-day periods.

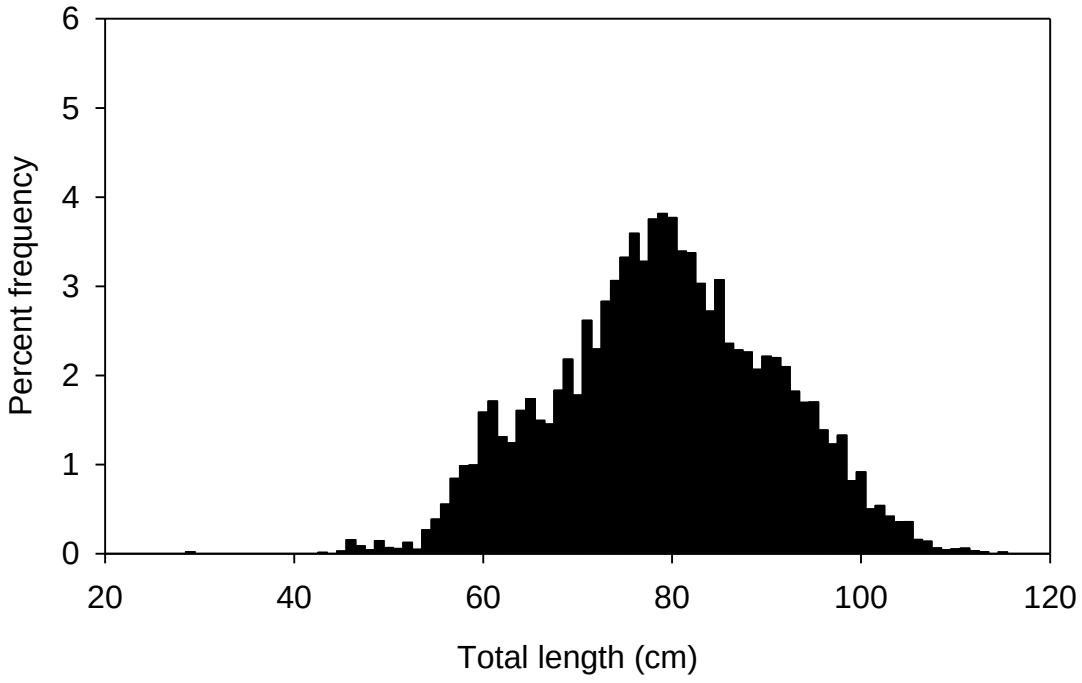

Figure 4: Scaled unsexed length frequency distribution of hoki caught in the commercial fishery in Cook Strait in 2017 based on at-sea observer sampling and land-based sampling. Data were used to estimate the ratio, *r*, of mean weight to mean backscattering cross-section for Cook Strait hoki.

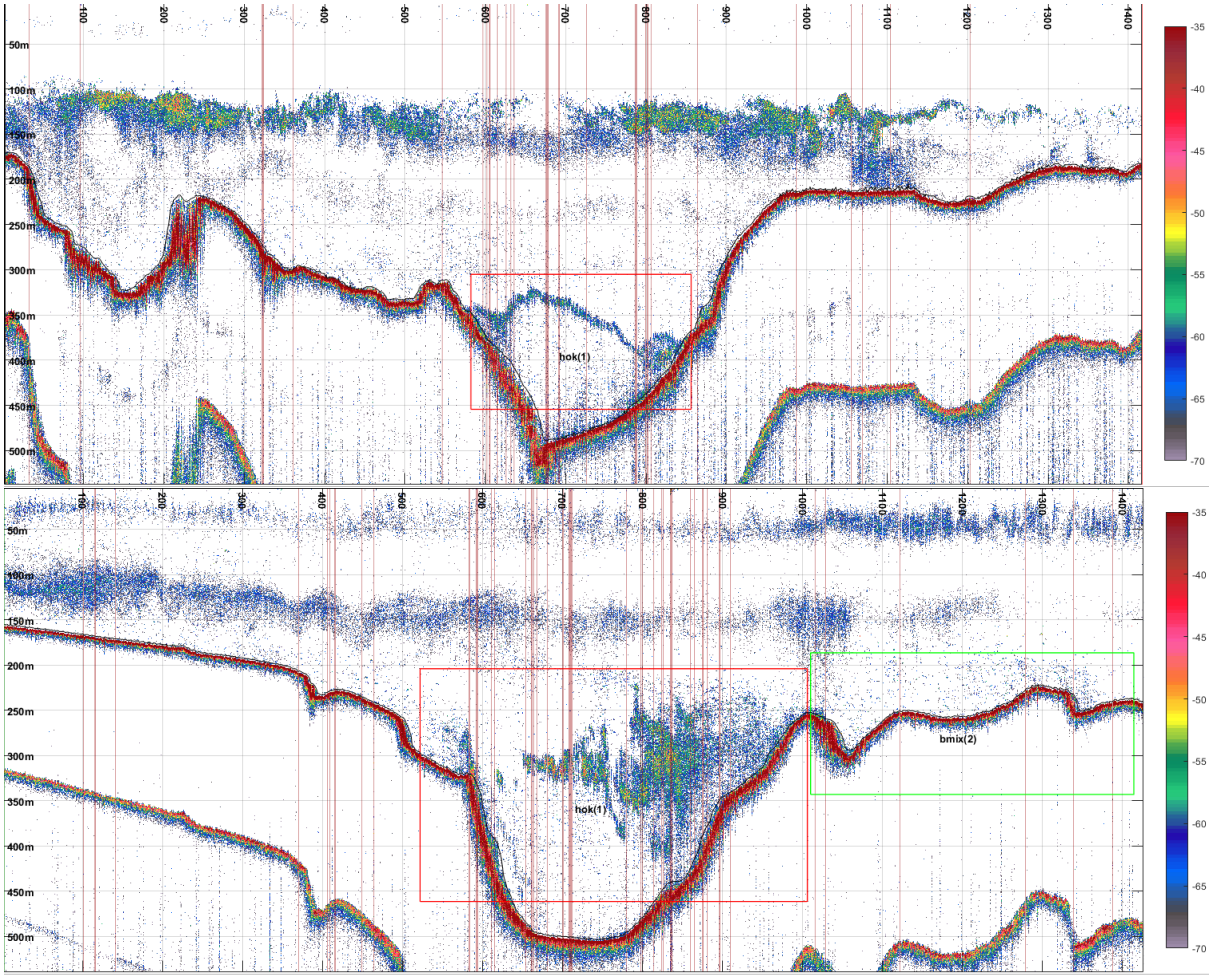

Figure 5: Acoustic echograms from Cook Strait Canyon (stratum 2) collected during snapshot 3 (upper panel) and snapshot 4 (lower panel) Red vertical lines mark missing data due to wave-generated bubbles. Layers from 100–200 m are probably mesopelagic fish.

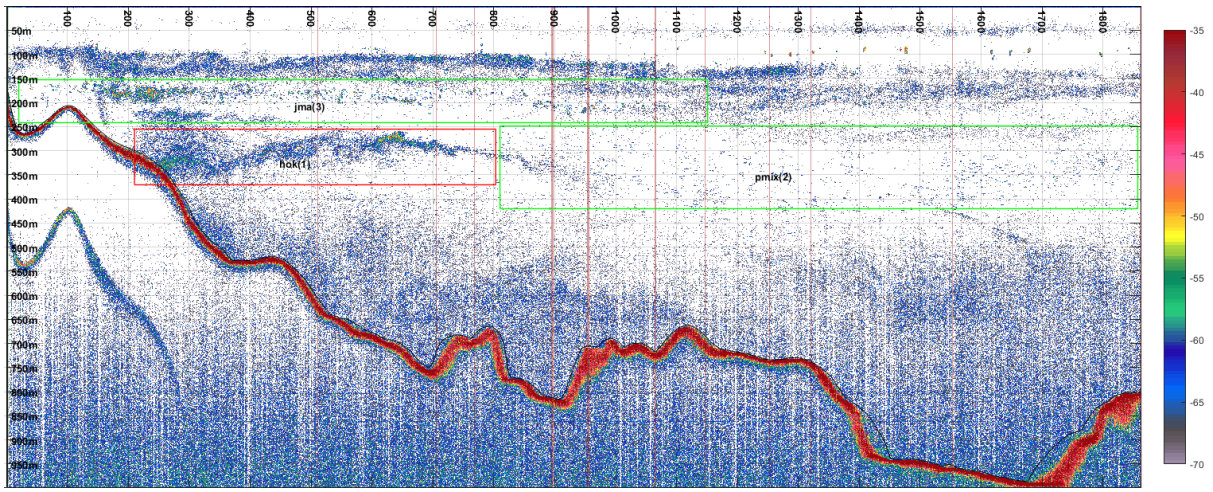

Figure 6: Acoustic echogram from deepwater between Cook and Wairarapa Canyons (stratum 5B) during snapshot 5 showing hoki schools (red box) in midwater. Layer from 100-200 m is probably mesopelagic fish. Blue colouration below 600 m depth is noise due to vessel and flow.

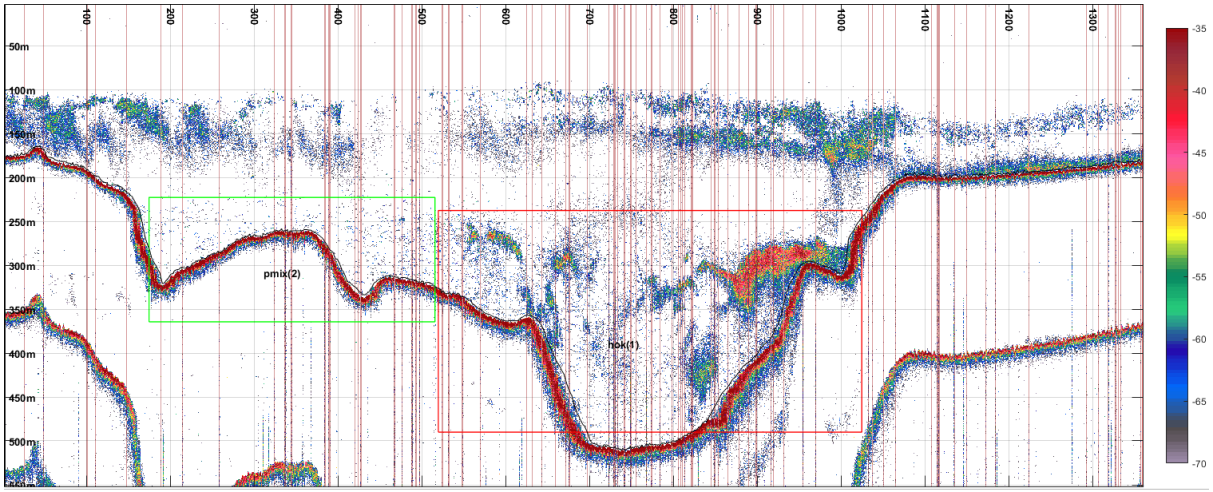

Figure 7: Acoustic echogram from Cook Strait Canyon (stratum 2) during snapshot 2 showing a very dense hoki school (red rectangle labelled 'hok'). Dispersed pelagic fuzz ('pmix') layers occur to the left (green rectangle). Layer from 100-200 m is probably mesopelagic fish.

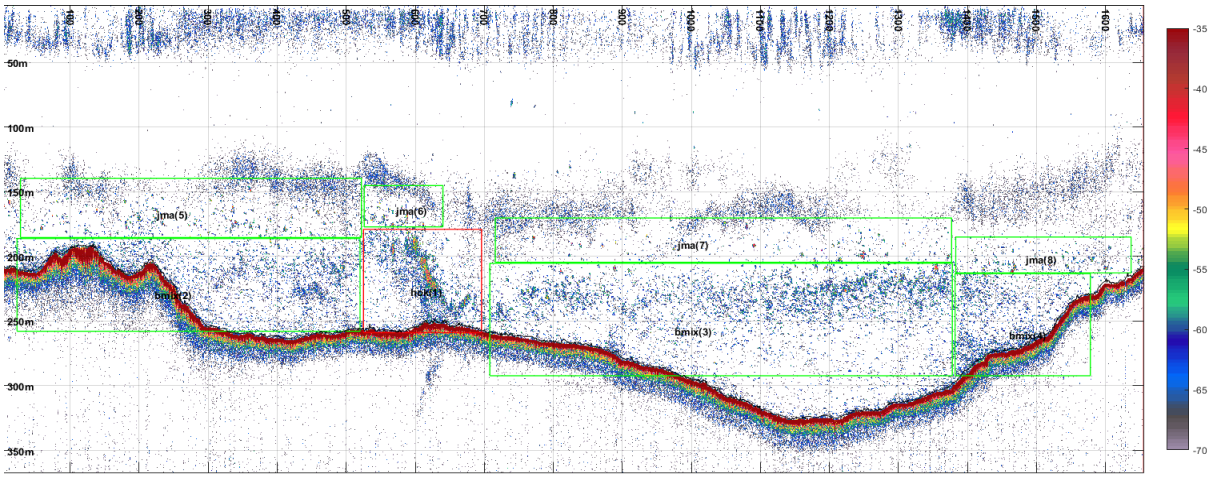

Figure 8: Acoustic echogram from Narrows Basin (stratum 1) during snapshot 3 showing small hoki school (red box) and hoki bottom fuzz within 100 m of the bottom (green rectangles labelled 'bmix') and small jack mackerel schools ('jma') above.

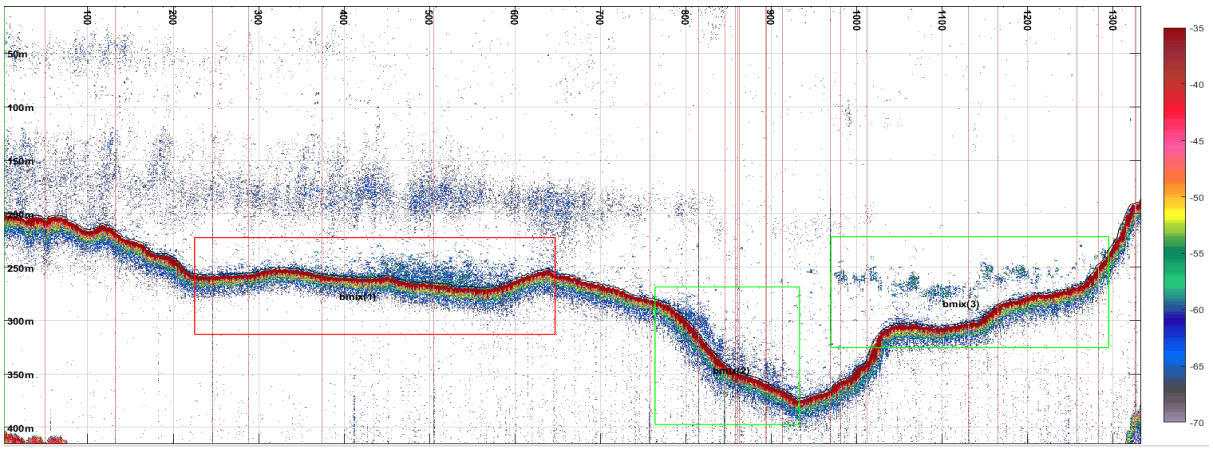

Figure 9: Acoustic echogram from Narrows Basin (stratum 1) during snapshot 5 showing other examples of hoki bottom fuzz.

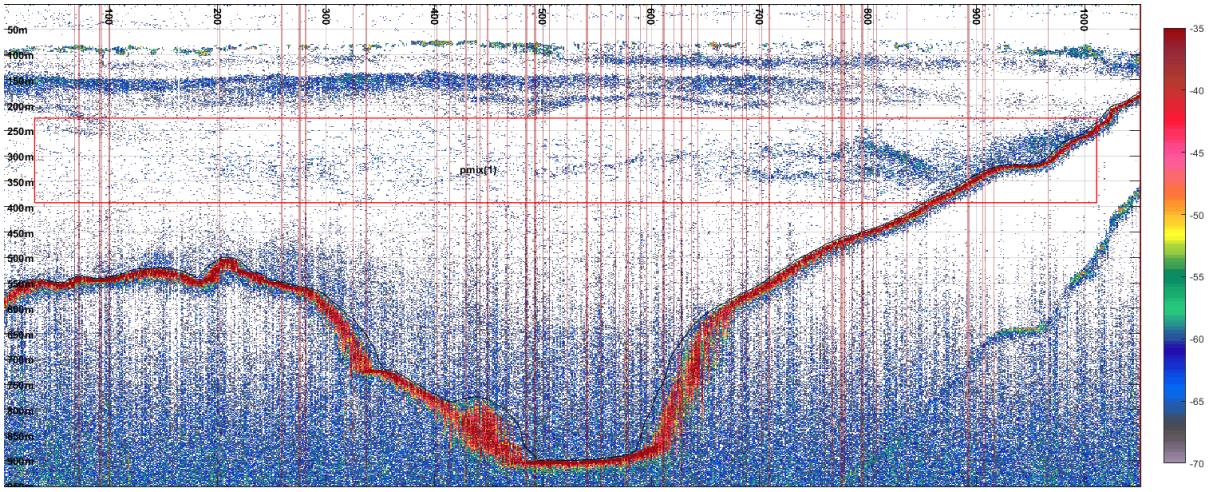

Figure 10: Acoustic echogram from outer Cook Strait (stratum 5A) during snapshot 6 showing dispersed hoki pelagic fuzz marks (red rectangle labelled 'pmix'). The layers above are probably mesopelagic fish.

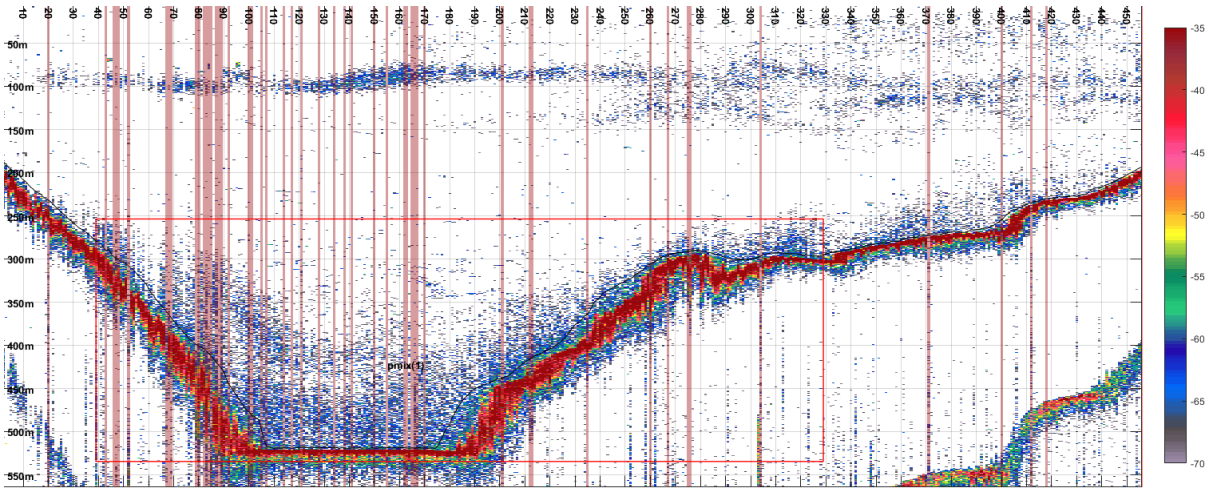

Figure 11: Acoustic echogram from Nicholson Canyon (stratum 3) during snapshot 5 showing another example of dispersed hoki fuzz marks (red rectangle).

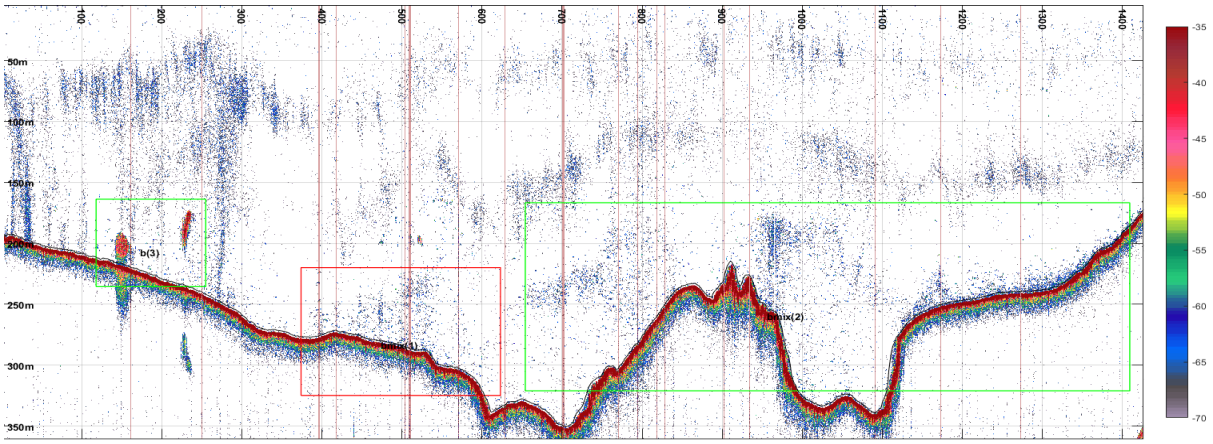

Figure 12: Acoustic echogram from Narrows Basin (stratum 1) during snapshot 5 showing dense bottom (non-hoki) marks (left-hand green rectangle).

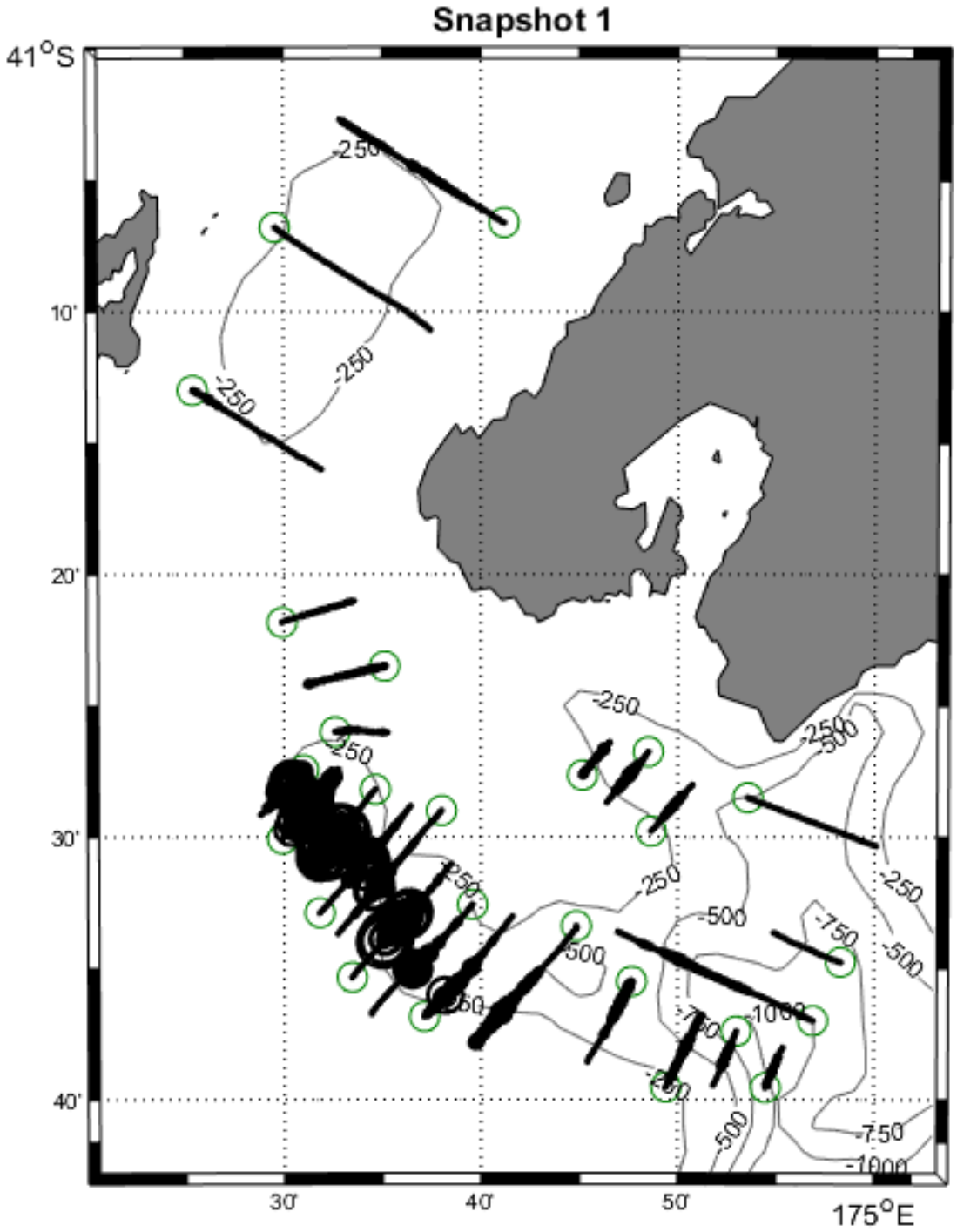

Figure 13: Spatial distribution of hoki acoustic backscatter density calculated from echo integration in bins of 10 ping (about 100 m) for snapshot 1 in 2017. Circle area is proportional to the acoustic backscatter density. Green circles show the start of each transect.

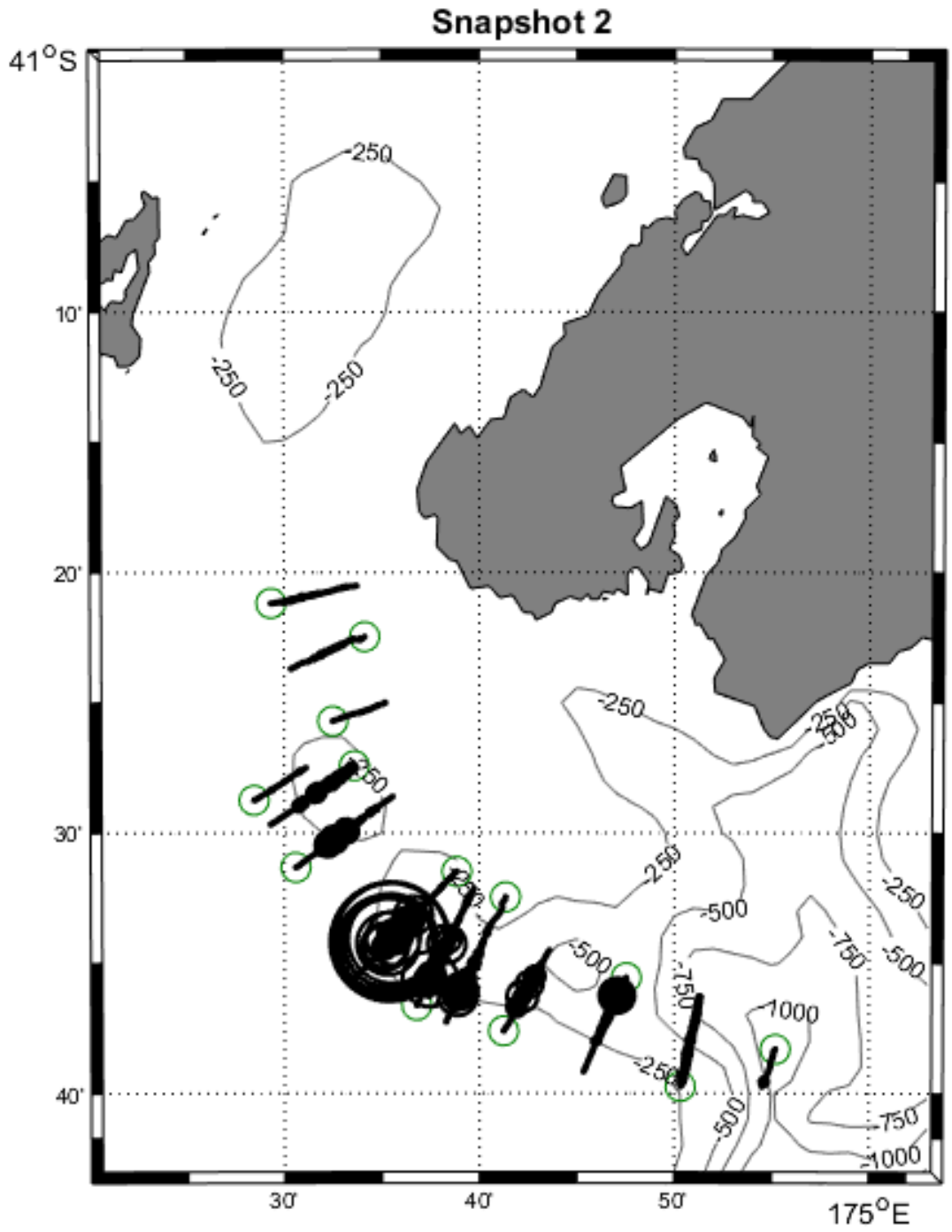

Figure 13 cntd: Spatial distribution of hoki acoustic backscatter density calculated from echo integration in bins of 10 ping (about 100 m) for snapshot 2 in 2017. Circle area is proportional to the acoustic backscatter density. Green circles show the start of each transect.

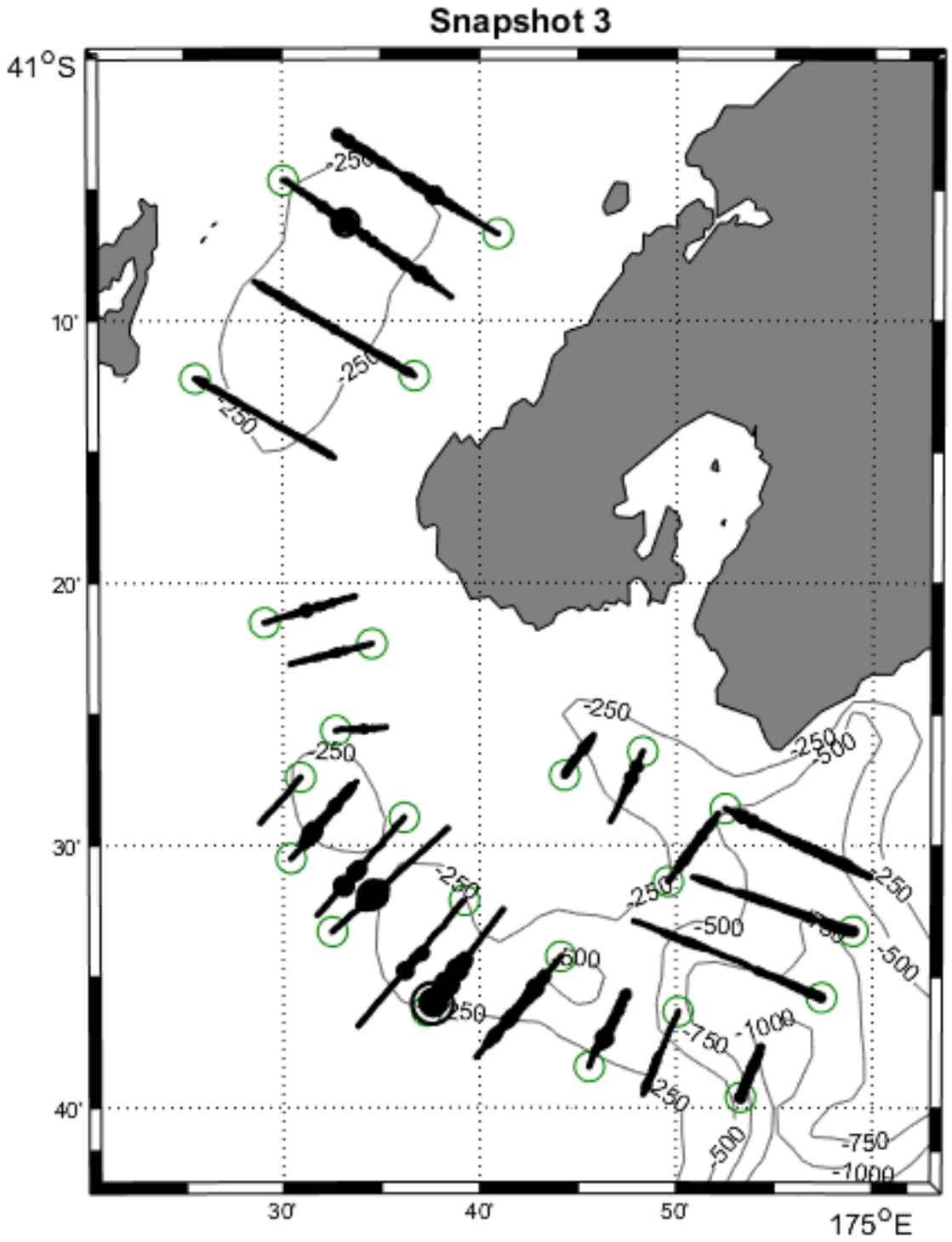

Figure 13 cntd: Spatial distribution of hoki acoustic backscatter density calculated from echo integration in bins of 10 ping (about 100 m) for snapshot 3 in 2017. Circle area is proportional to the acoustic backscatter density. Green circles show the start of each transect.

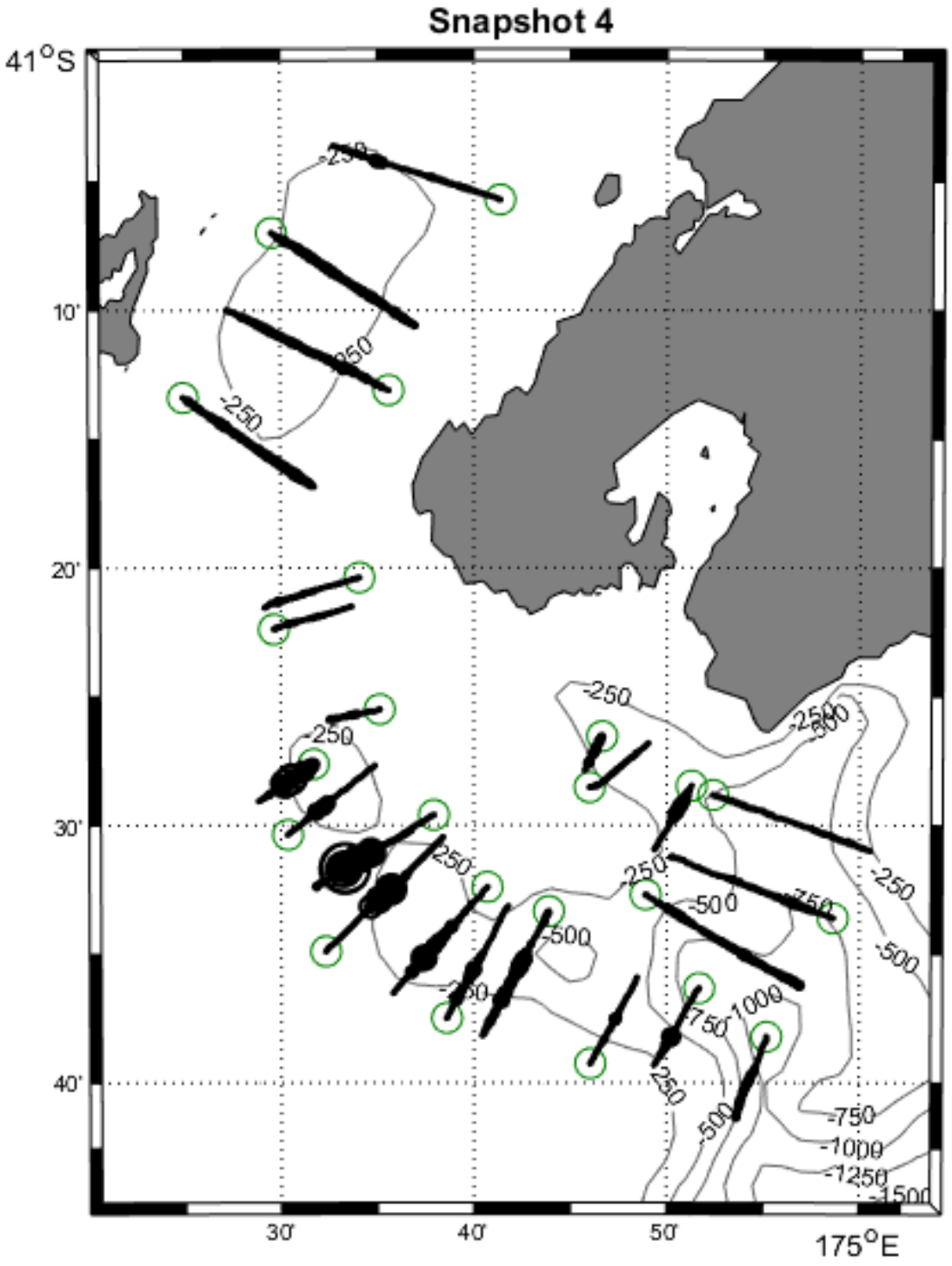

Figure 13 cntd: Spatial distribution of hoki acoustic backscatter density calculated from echo integration in bins of 10 ping (about 100 m) for snapshot 4 in 2017. Circle area is proportional to the acoustic backscatter density. Green circles show the start of each transect.

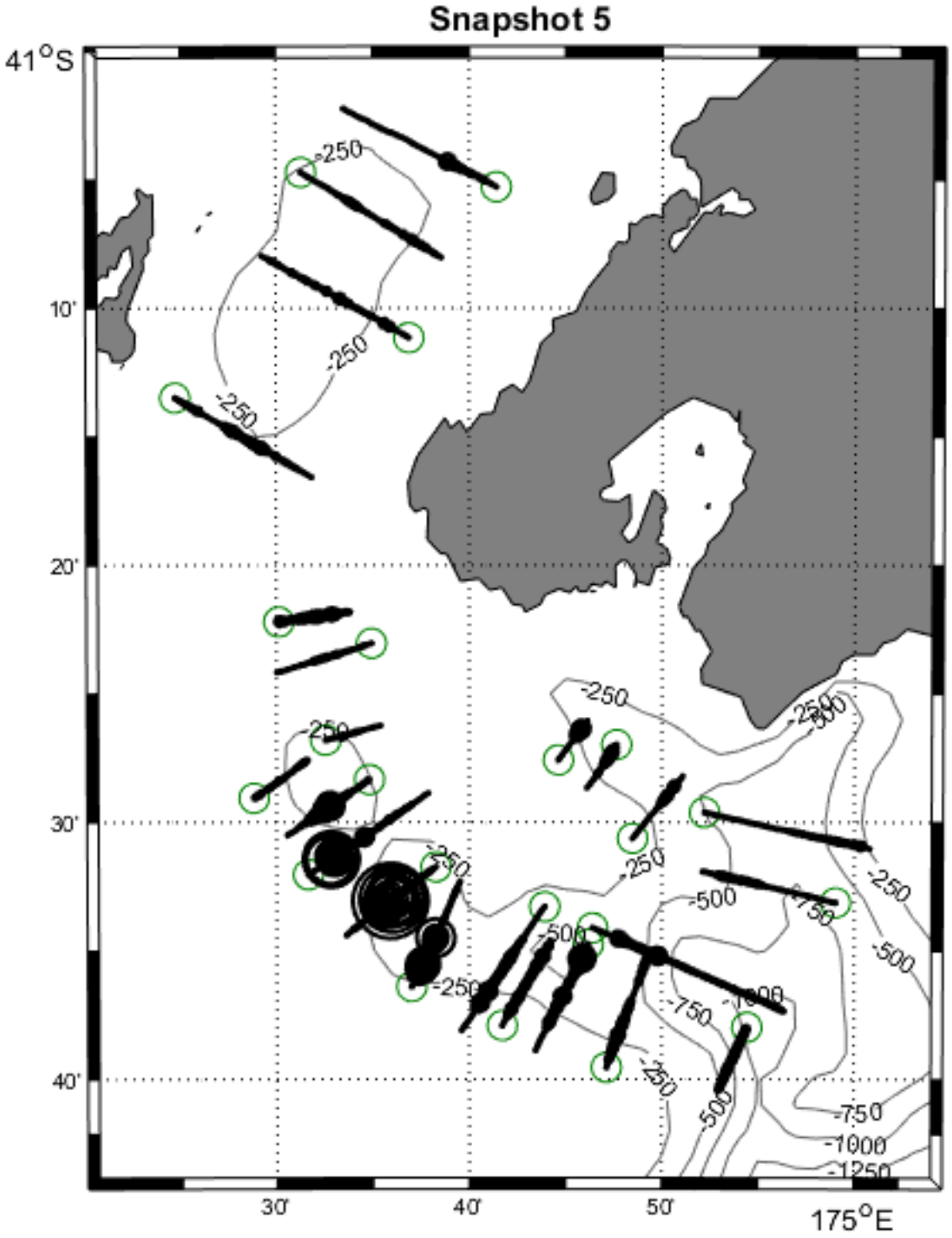

Figure 13 cntd: Spatial distribution of hoki acoustic backscatter density calculated from echo integration in bins of 10 ping (about 100 m) for snapshot 5 in 2017. Circle area is proportional to the acoustic backscatter density. Green circles show the start of each transect.

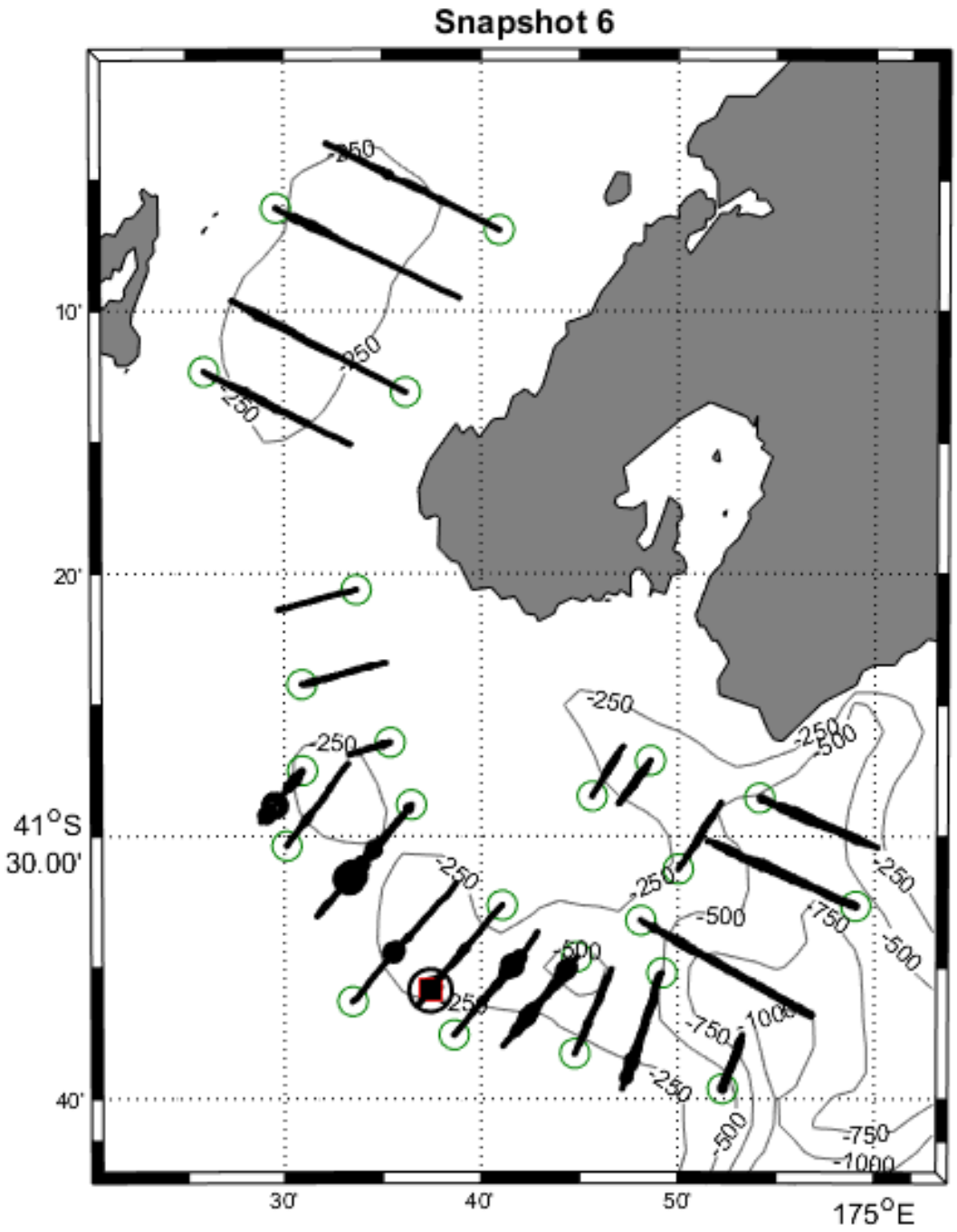

Figure 13 cntd: Spatial distribution of hoki acoustic backscatter density calculated from echo integration in bins of 10 ping (about 100 m) for snapshot 6 in 2017. Circle area is proportional to the acoustic backscatter density. Green circles show the start of each transect.

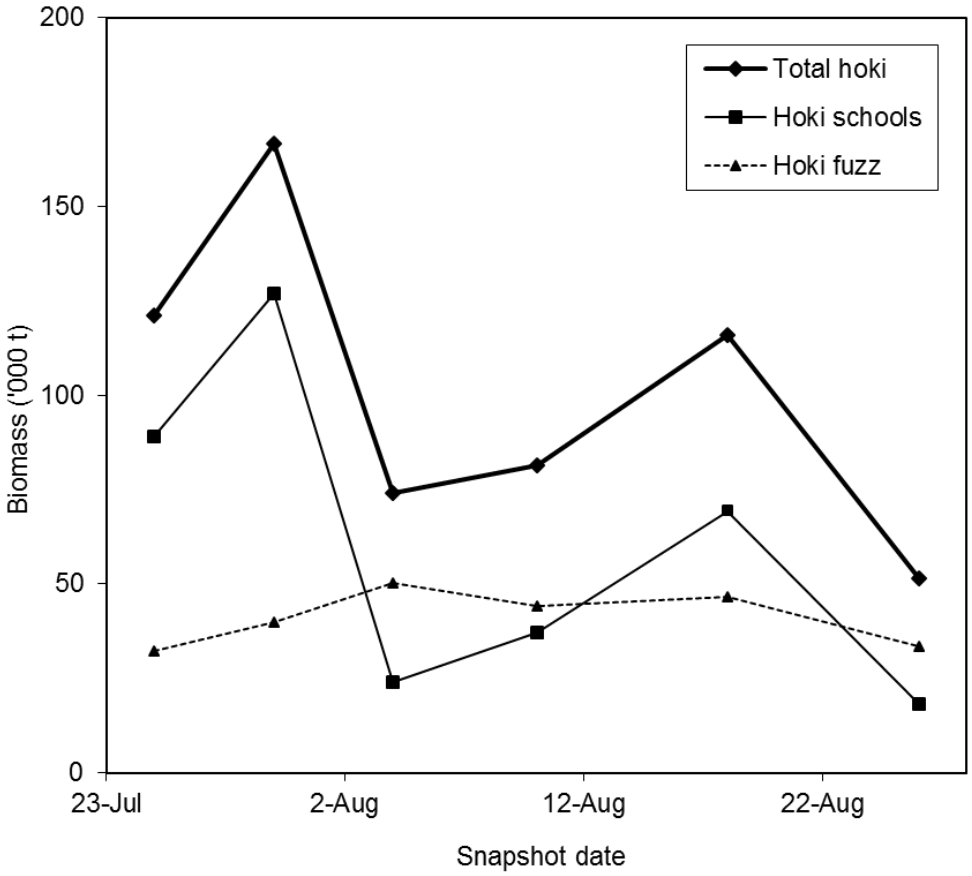

Figure 14: Estimated hoki abundance in Cook Strait by snapshot and mark type from the 2017 survey.

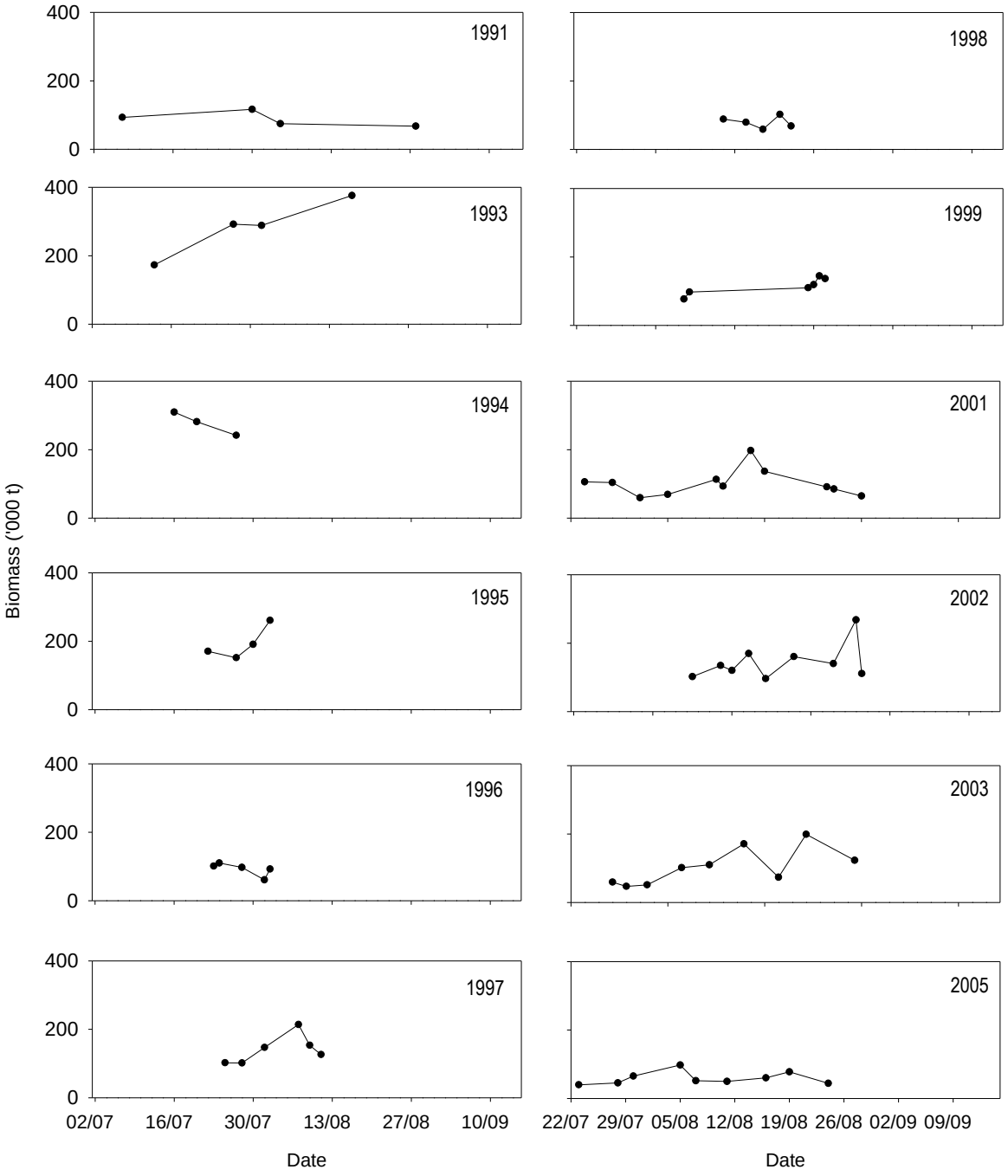

Figure 15: Estimated hoki abundance by snapshot for acoustic surveys in the Cook Strait time series from 1991 to 2005.

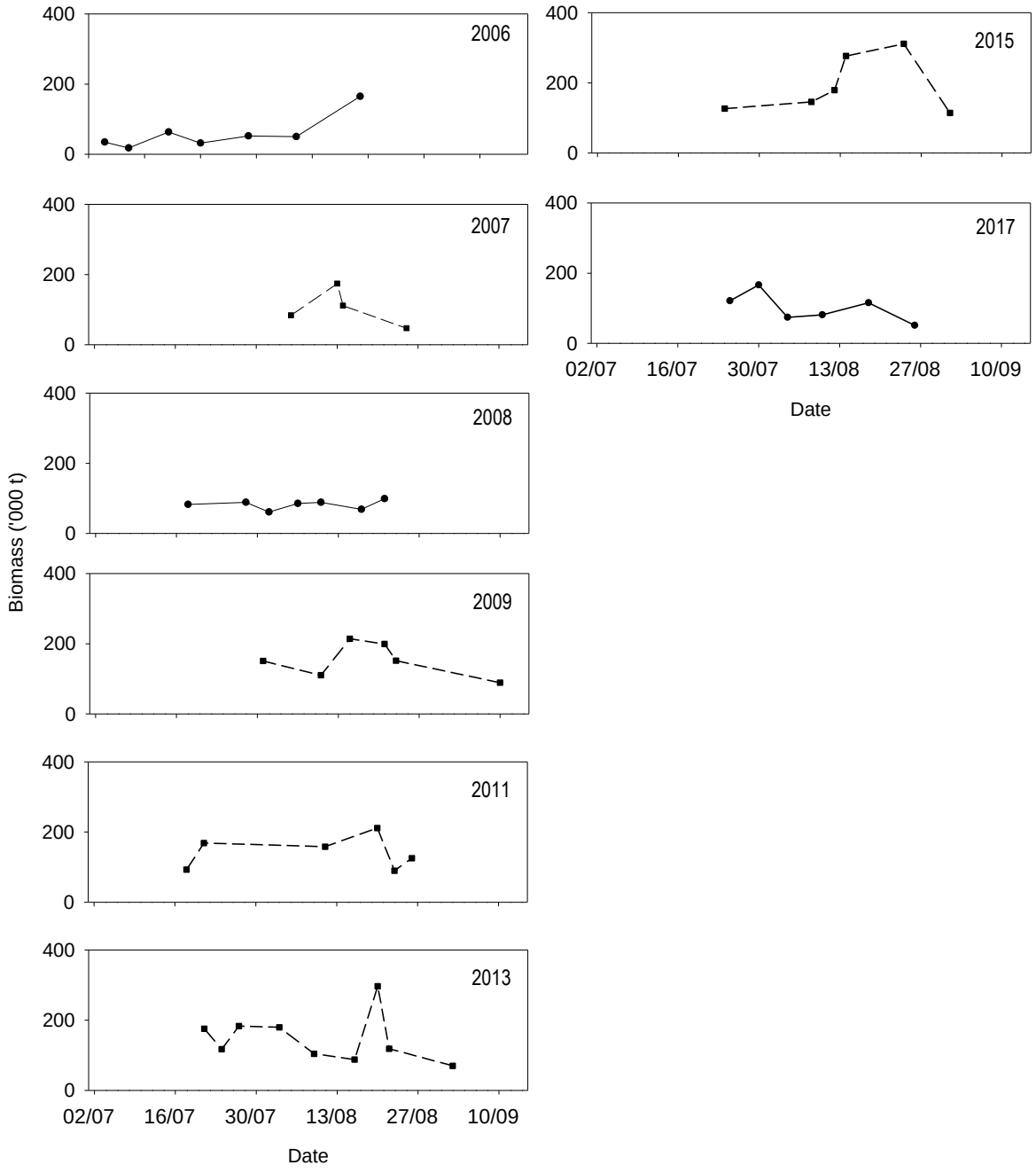

Figure 15 cntd: Estimated hoki abundance by snapshot for acoustic surveys in the Cook Strait time series from 2006 to 2017. Dotted lines show surveys carried out from commercial vessels.

APPENDIX 1: Calibration Report *Ikatere* 20 July 2017

A portable Simrad EK60 echosounder was installed on *Ikatere* for the 2017 hoki acoustic survey in Cook Strait (Ministry for Primary Industries research project HOK2017/01). The ES38D transducer from Towbody3 was mounted on a pole which allowed it to be raised and lowered through the moon-pool in the centre of the vessel (Figure A1.1). When deployed, the transducer was approximately 1 m below the surface below and aft of the foil between the two hulls.

Calibration of the echosounder took place in Wellington Harbour in the hole near Somes Island (41° 15.9' S 174° 51.9' E) on 20 July 2017. Water depth was about 27 m (below the transducer). The calibration was carried out by Richard O'Driscoll, Pablo Escobar-Flores, Peter de Joux, and Alexandre Schimel (NIWA) following the procedures in Demer et al. (2015).

There have been no previous calibrations of this GPT and transducer combination. The GPT was previously used with a hull-mounted transducer on *Amaltal Mariner* in May–July 2017, and the transducer was used with the GPT in towbody 3 (most recent calibration on 7 September 2016).

NIWA staff boarded *Ikatere* at 11:00 NZST at Evans Bay Marina. The vessel departed at 12:00. The EK60 was configured to Cook Strait survey settings (see Table A1.1) and the PC time was set to the GPS before the calibration began. The ER60 software was running off a NUC running Windows 10, using the large TV screen available on *Ikatere*. Position and pitch-roll data were available from a POS-MV system connected to serial port 3 with baud rate of 19200. All systems were powered from the vessel's generator. It was noted that the ER60 software in Windows 10 did not correctly save all configuration settings on exit. The maximum ping rate was also much slower than expected (only 2 pings per second with 30 m record range).

The vessel was anchored to avoid drifting out of the deeper hole, and the calibration commenced at 12:20 NZST. A weighted line was passed under the keel to facilitate setting up the three lines and calibration sphere. Long (3.8 m) fibreglass calibration poles were used to help keep the calibration lines clear of the hull. Pole positions are shown in Figure A1.2. The sphere and associated lines were immersed in a soap solution prior to entering the water. A lead weight was also deployed about 3 m below the sphere to steady the arrangement of lines. The sphere was centred in the beam, and was then moved around the beam to obtain data for the beam shape calibration.

The weather was good with 10 knots northeast winds and no swell. The vessel was swinging slowly at anchor. The sphere was located in the beam at 12:32 and calibration data were collected until 14:02 in three EK60 ".raw" format files (ika1701-D20170720-T003004, ika1701-D20170720-T004830, ika1701-D20170720-T013245). Raw data are stored on the NIWA *acoustics* sever.

Before leaving the calibration site, water temperature measurements were taken using an RBR Duet temperature depth probe, serial number 82705. The water column was unstratified, with a mean temperature of 10.54º. The salinity was not measured and was assumed to be 35 PSU. An estimate of acoustic absorption was calculated using the formulae in Doonan et al. (2003) and an estimate of sound speed was calculated using the formulae of Fofonoff & Millard (1983).

After the calibration, the *Ikatere* steamed into Cook Strait to carry out noise trials in deep water, before returning to Evans Bay, and berthing at about 16:30.

The data in the EK60 files were extracted using custom-written ESP3 software. The amplitude of the sphere echoes was obtained by filtering on range, and choosing the sample with the highest amplitude. Instances where the sphere echo was disturbed by fish echoes were discarded. The alongship and athwartship beam widths and offsets were calculated by fitting the sphere echo amplitudes to the Simrad theoretical beam pattern:

$$compensation = 6.0206\left(\left(\frac{2\theta_{fa}}{BW_{fa}}\right)^2 + \left(\frac{2\theta_{ps}}{BW_{ps}}\right)^2 - 0.18\left(\frac{2\theta_{fa}}{BW_{fa}}\right)^2\left(\frac{2\theta_{ps}}{BW_{ps}}\right)^2\right),$$

where θ_{ps} is the port/starboard echo angle, θ_{fa} the fore/aft echo angle, BW_{ps} the port/starboard beamwidth, BW_{fa} the fore/aft beamwidth, and *compensation* the value, in dB, to add to an uncompensated echo to yield the compensated echo value. The fitting was done using an unconstrained nonlinear optimisation (as implemented by the Matlab fminsearch function). The Sa correction was calculated from:

$$S_{a,corr} = 5\log_{10}\left(\frac{\sum P_i}{4P_{\max}}\right),$$

where P_i is the sphere echo power measurement and P_{max} the maximum sphere echo power measurement. A value for $S_{a,corr}$ is calculated for all valid sphere echoes and the mean over all sphere echoes is used to determine the final $S_{a,corr}$.

Results

The mean range of the sphere and the sound speed and acoustic absorption between the transducer and the sphere are given in Table A1.2.

The calibration results are given in Table A1.3. The estimated beam pattern and sphere coverage are shown in Figure A1.3. The symmetrical nature of the pattern and the zero centre of the beam pattern indicate that the transducer and transceiver were operating correctly. The fits between the theoretical beam pattern and the sphere echoes are shown in Figure A1.4 and confirms that the transducer beam pattern is correct. The RMS of the difference between the Simrad beam model and the sphere echoes out to 3.5° off axis was 0.10 dB (Table A1.3), indicating that the calibration was of excellent quality (>0.4 dB is poor, 0.2–0.3 dB good, and <0.2 dB excellent). The estimated peak gain (G_0) was 25.38 dB and the sa correction was -0.65 dB.

Table A1.1. EK60 transceiver settings and other relevant parameters during the calibration.

Parameter	Value
Echosounder	Portable EK60
ER60 software version	2.4.3
Transducer model	ES38D
Transducer serial number	28332B
EK60 GPT serial number	009072058c97
GPT software version	070413
Sphere type/size	tungsten carbide/38.1 mm diameter
Operating frequency (kHz)	38
Transducer depth (m)	1
Transmit power (W)	2000
Pulse length (ms)	1.024
Transducer peak gain (dB)	26.5
Sa correction (dB)	0.0
Bandwidth (Hz)	2425
Sample interval (m)	0.192
Two-way beam angle (dB)	–20.60
Absorption coefficient (dB/km)	9.75
Speed of sound (m/s)	1500
Angle sensitivity (dB) alongship/athwartship	21.90/21.90
3 dB beamwidth (º) alongship/athwartship	7.10/7.10
Angle offset (º) alongship/athwartship	0.0/0.0

Table A1.2: Auxiliary calibration parameters derived from depth and temperature measurements.

Parameter	Value
Mean sphere range (m)	17.05
S.D. of sphere range (m)	0.93
Mean sound speed (m/s)	1 492
Mean temperature (°C)	10.54
Mean absorption (dB/km)	9.52
Sphere TS (dB re 1m^2)	–42.40

Table A1.3: Calculated echosounder calibration parameters. Values were calculated using ESP3 software version 0.6.1.0.

Parameter	Value
Mean TS within 0.21° of centre	-44.65
Std dev of TS within 0.21° of centre	0.14
Max TS within 0.21° of centre	-44.34
No. of echoes within 0.21° of centre	101
On axis TS from beam-fitting	-44.50
Transducer peak gain (dB) mean TS	25.38
Sa correction (dB)	-0.65
Beamwidth (º) along/athwartship	7.26/7.04
Beam offset (º) along/athwartship	0.01/-0.02
RMS deviation	0.11
Number of echoes	4 309

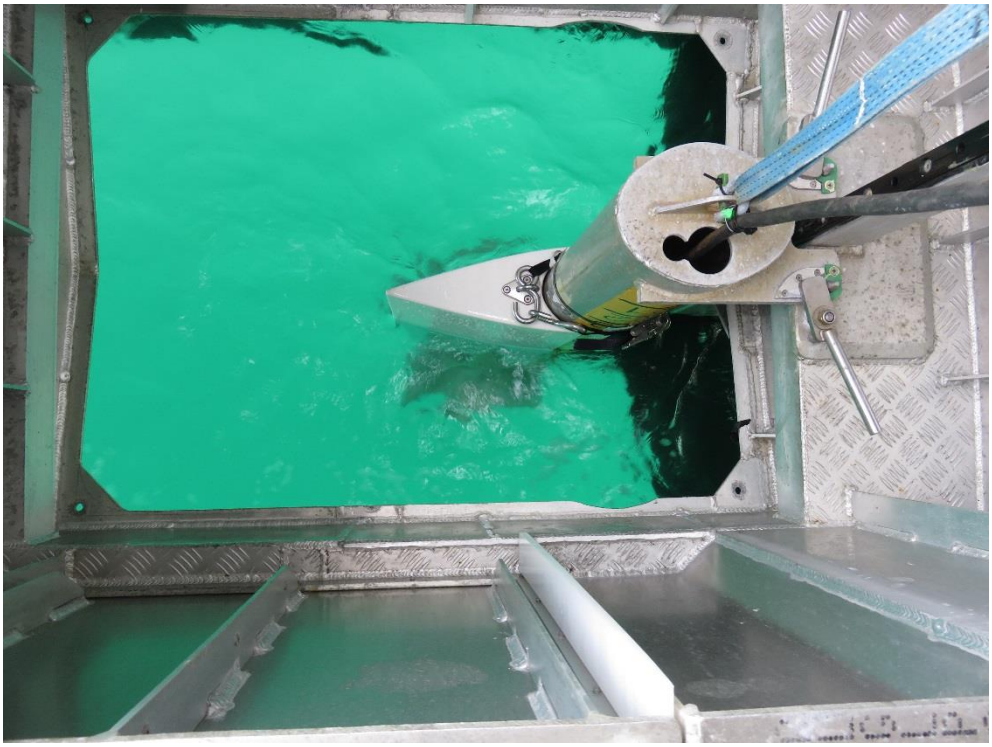

Figure A1.1: Picture showing deployment of pole-mounted ES38D transducer through moon-pool on *Ikatere*.

Port side in line with transducer

Figure A1.2: Pole positions for calibration of pole-mounted transducer on *Ikatere*.

Starboard aft

Starboard forward

Figure A1.2 cntd. Pole positions for calibration of pole-mounted transducer on *Ikatere*.

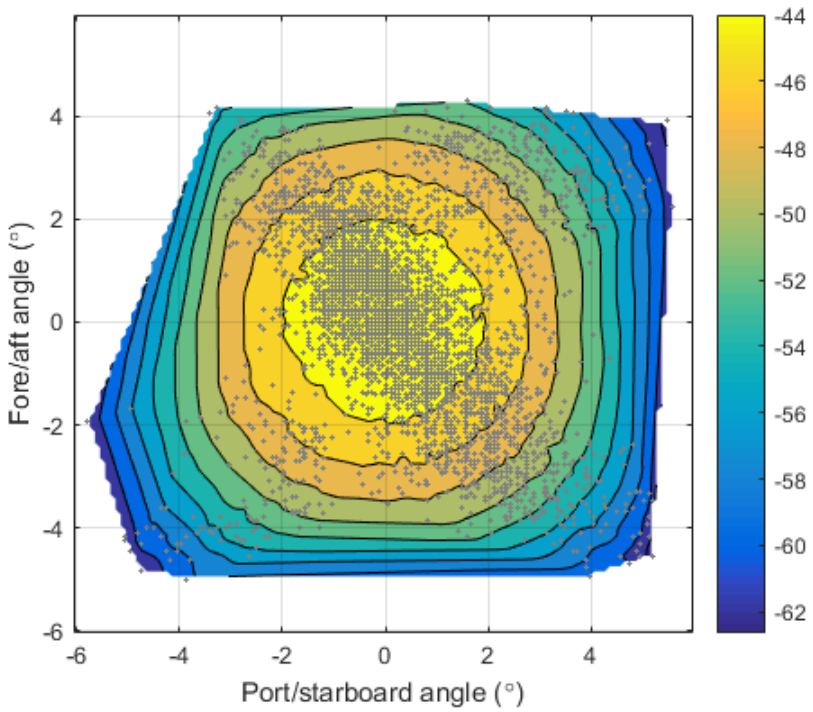

Figure A1.3: The estimated beam pattern from the sphere echo strength and position for the calibration. The '+' symbols indicate where sphere echoes were received. The colours indicate the received sphere echo strength in dB re 1 m^2.

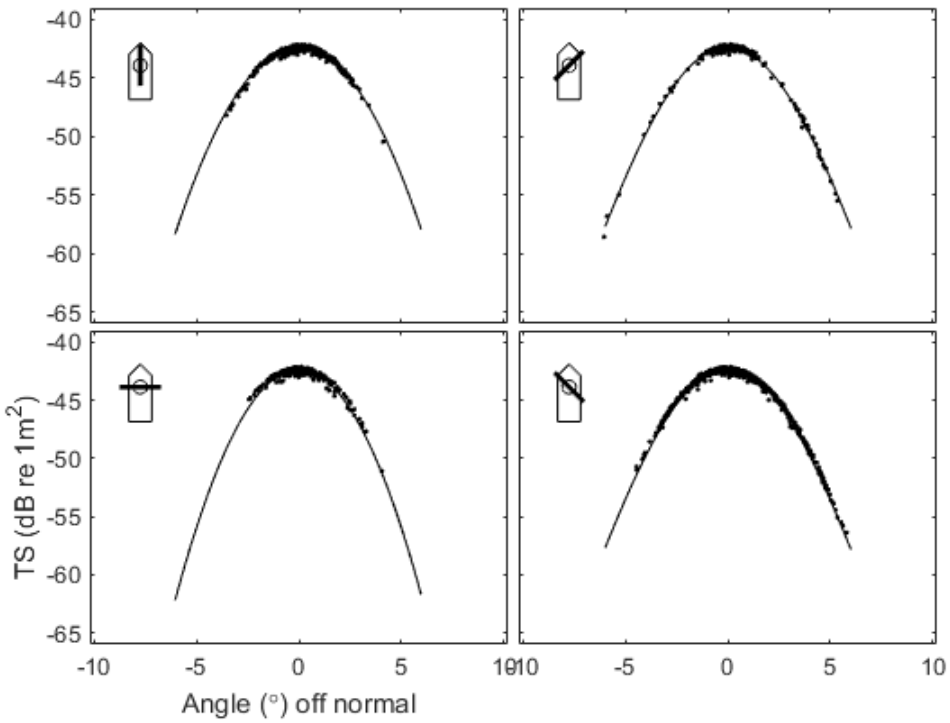

Figure A1.4: Beam pattern results from the calibration analysis. The solid line is the theoretical beam pattern fit to the sphere echoes for four slices through the beam.

APPENDIX 2: Calibration Report *Ikatere* 23 August 2017

The second calibration of the portable Simrad EK60 echosounder installed on *Ikatere* for the 2017 hoki acoustic survey in Cook Strait (Ministry for Primary Industries research project HOK2017/01) took place in Wellington Harbour in the hole near Somes Island (41° 15.9' S 174° 51.9' E) on 23 August 2017. Water depth was about 27.5 m (below the transducer). The calibration was carried out by Pablo Escobar-Flores, Yoann Ladroit and Nick Eton (NIWA) following the procedures in Demer et al. (2015).

NIWA staff boarded *Ikatere* at 07:10 NZST at Evans Bay Marina. The vessel departed at 08:30. The EK60 was configured to Cook Strait survey settings (see Table A2.1) and the PC time was set to the GPS before the calibration began. Due to the addition of a 30 cm extension to the pole, the transducer was approximately 1.3 m below the surface when deployed below and aft of the foil between the two hulls. ER60 software was running off a NIWA laptop running Windows 10. This allowed a much faster ping rate to be achieved compared to the first calibration where the ER60 software was running of a NUC which limited the maximum ping rate.

The vessel was anchored to avoid drifting out of the deeper hole, and the calibration commenced at 09:35 NZST. A weighted line was passed under the keel to facilitate setting up the three lines and calibration sphere. Long (3.8 m) fibreglass calibration poles were used to help keep the calibration lines clear of the hull. Pole positions were identical to those in calibration 1 (see Figure A1.2). The sphere and associated lines were immersed in a soap solution prior to entering the water. A lead weight was also deployed about 3 m below the sphere to steady the arrangement of lines. The sphere was centred in the beam, and was then moved around the beam to obtain data for the beam shape calibration. Due to the strong water current, poles were removed from their fixed positions during the calibration and held by NIWA staff in different positions of the vessel to increase the number of targets in the centre of the beam for on-axis calibration, and to achieve a good coverage of targets in the beam for estimating beam pattern.

The weather was acceptable with 10–15 knots southerly winds and no swell. The vessel was swinging slowly at anchor. The sphere was located in the beam at 09:37 and calibration data were collected until 10:29 in four EK60 ".raw" format files (ika1701-D20170822-T213838, ika1701-D20170822-T220606, ika1701-D20170822-T221958 and ika1701-D20170822-T222927). Raw data are stored on the NIWA *acoustics* sever.

Before leaving the calibration site, water temperature measurements were taken using an RBR Duet temperature depth probe, serial number 82705. The water column was unstratified, with a mean temperature of 11.57 ºC. The salinity was not measured and was assumed to be 35 PSU. An estimate of acoustic absorption was calculated using the formulae in Doonan et al. (2003) and an estimate of sound speed was calculated using the formulae of Fofonoff & Millard (1983).

After the calibration, the *Ikatere* steamed into Cook Strait to test the NIWA AOS, before returning to Evans Bay and berthing at about 15:30.

The data in the EK60 files were extracted using custom-written ESP3 software. The amplitude of the sphere echoes was obtained by filtering on range, and choosing the sample with the highest amplitude. Instances where the sphere echo was disturbed by fish echoes were discarded. The alongship and athwartship beam widths and offsets were calculated by fitting the sphere echo amplitudes to the Simrad theoretical beam pattern:

$$compensation = 6.0206\left(\left(\frac{2\theta_{fa}}{BW_{fa}}\right)^2 + \left(\frac{2\theta_{ps}}{BW_{ps}}\right)^2 - 0.18\left(\frac{2\theta_{fa}}{BW_{fa}}\right)^2\left(\frac{2\theta_{ps}}{BW_{ps}}\right)^2\right),$$

where θ_{ps} is the port/starboard echo angle, θ_{fa} the fore/aft echo angle, BW_{ps} the port/starboard beamwidth, BW_{fa} the fore/aft beamwidth, and *compensation* the value, in dB, to add to an

uncompensated echo to yield the compensated echo value. The fitting was done using an unconstrained nonlinear optimisation (as implemented by the Matlab fminsearch function). The Sa correction was calculated from:

$$S_{a,corr} = 5\log_{10}\left(\frac{\sum P_i}{4P_{\max}}\right),$$

where P_i is the sphere echo power measurement and P_{max} the maximum sphere echo power measurement. A value for $S_{a,corr}$ is calculated for all valid sphere echoes and the mean over all sphere echoes is used to determine the final $S_{a,corr}$.

Results

The mean range of the sphere and the sound speed and acoustic absorption between the transducer (1-1.5 m deep) and the sphere are given in Table A2.2.

The calibration results are given in Table A2.3. The estimated beam pattern and sphere coverage are shown in Figure A2.1. The asymmetrical pattern observed in the port fore quadrant of the beam pattern was due to the strong current which dragged the sphere starboard aft. The zero centre of the beam pattern indicated that the transducer and transceiver were operating correctly. The fits between the theoretical beam pattern and the sphere echoes are shown in Figure A2.2 and confirms that the transducer beam pattern is correct. The RMS of the difference between the Simrad beam model and the sphere echoes out to 3.5° off axis was 0.09 dB (Table A2.3), indicating that the calibration was of excellent quality (>0.4 dB is poor, 0.2–0.3 dB good, and <0.2 dB excellent). The estimated peak gain (G_0) was 25.59 dB and the sa correction was -0.63 dB (Table A2.3). The G_0 was 0.21 dB higher than that estimated using the same system a month earlier in the first calibration (Appendix 1).

Table A2.1. EK60 transceiver settings and other relevant parameters during the calibration.

Parameter	Value
Echosounder	Portable EK60
ER60 software version	2.4.3
Transducer model	ES38D
Transducer serial number	28332B
EK60 GPT serial number	009072058c97
GPT software version	070413
Sphere type/size	tungsten carbide/38.1 mm diameter
Operating frequency (kHz)	38
Transducer depth (m)	1
Transmit power (W)	2000
Pulse length (ms)	1.024
Transducer peak gain (dB)	26.5
Sa correction (dB)	0.0
Bandwidth (Hz)	2425
Sample interval (m)	0.192
Two-way beam angle (dB)	–20.60
Absorption coefficient (dB/km)	9.75
Speed of sound (m/s)	1500
Angle sensitivity (dB) alongship/athwartship	21.90/21.90
3 dB beamwidth (º) alongship/athwartship	7.10/7.10
Angle offset (º) alongship/athwartship	0.0/0.0

Table A2.2: Auxiliary calibration parameters derived from depth and temperature measurements.

Parameter	Value
Mean sphere range (m)	17.6
S.D. of sphere range (m)	2.9
Mean sound speed (m/s)	1 495
Mean temperature (°C)	11.52
Mean absorption (dB/km)	9.36
Sphere TS (dB re $1m^2$)	–42.41

Table A2.3: Calculated echosounder calibration parameters. Values were calculated using ESP3 software version 0.6.1.0.

Parameter	Value
Mean TS within 0.21° of centre	-44.22
Std dev of TS within 0.21° of centre	0.10
Max TS within 0.21° of centre	-43.97
No. of echoes within 0.21° of centre	58
On axis TS from beam-fitting	-44.13
Transducer peak gain (dB) mean TS	25.59
Sa correction (dB)	-0.63
Beamwidth (º) along/athwartship	7.25/7.03
Beam offset (º) along/athwartship	-0.08/-0.02
RMS deviation	0.10
Number of echoes	11 491

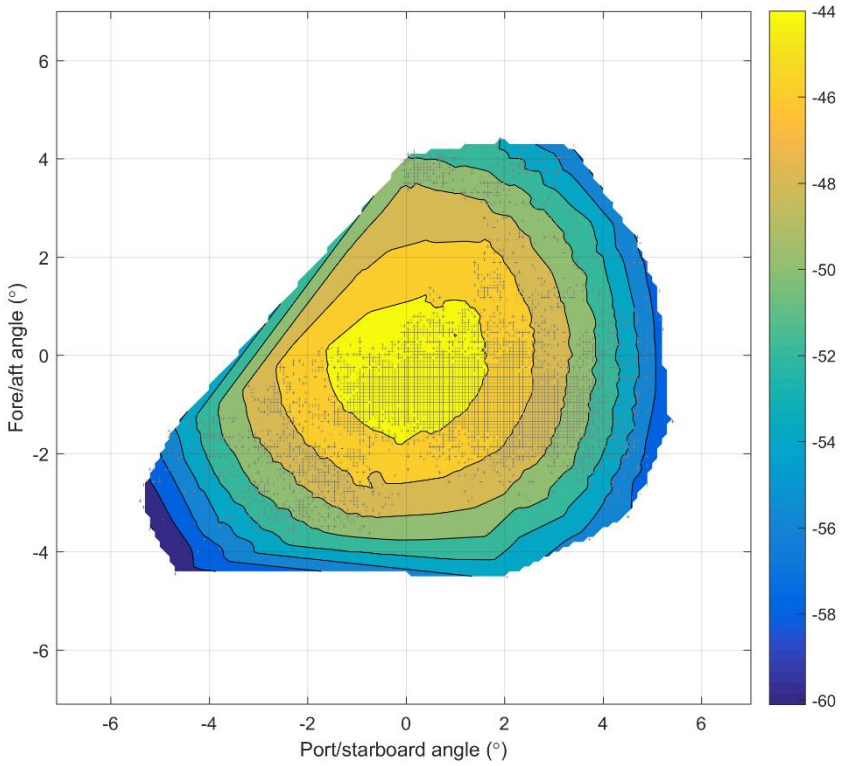

Figure A2.1: The estimated beam pattern from the sphere echo strength and position for the calibration. The '+' symbols indicate where sphere echoes were received. The colours indicate the received sphere echo strength in dB re 1 m^2.

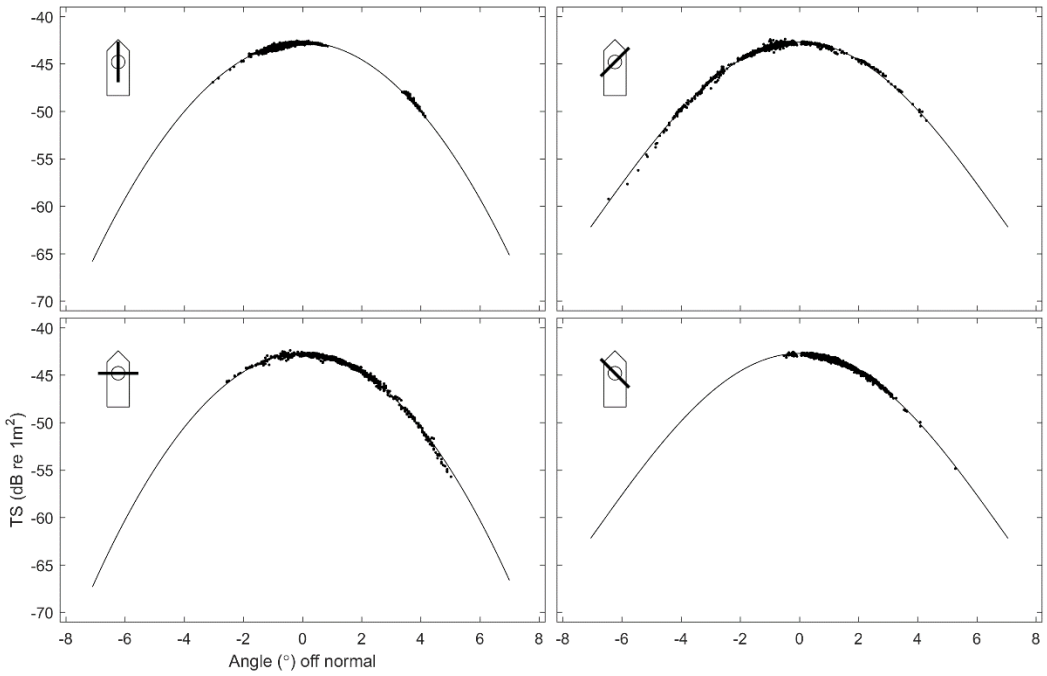

Figure A2.2: Beam pattern results from the calibration analysis. The solid line is the theoretical beam pattern fit to the sphere echoes for four slices through the beam.